# Dispersion theory of proton Compton scattering in the first and second resonance regions

A. I. L'vov* and V. A. Petrun'kin†
*P. N. Lebedev Physical Institute, Leninsky Prospect 53, Moscow 117924, Russia*

M. Schumacher‡
*II. Physikalisches Institut, Universität Göttingen, Bunsenstrasse 7-9, D-37073, Göttingen, Germany*
(Received 9 July 1996)

Dispersion theory of proton Compton scattering is extended to energies up to ~1 GeV where excitations of higher resonances and nonresonance double-pion photoproduction become important photoabsorption mechanisms. To saturate $s$-channel dispersion relations, the VPI partial-wave analysis of single-pion photoproduction and resonance photocouplings is used. Models for double-pion photoproduction and dispersion asymptotic contributions are constructed. The latter are mainly given by $\pi^0$ and $\sigma(600)$ exchanges. Being used in dispersion calculations, they result in a reasonable agreement with all available data on both differential cross sections and polarization observables in Compton scattering. Some unsolved problems are outlined. [S0556-2813(97)00401-9]

PACS number(s): 25.20.Dc, 11.55.Fv, 13.60.Fz, 13.60.Le

## I. INTRODUCTION

Probing nucleons with photons through elastic Compton scattering opens many interesting possibilities to learn about the structure of hadrons [1–3]. During the last years a lot of work has been done along this line and many experimental data [4–12] were obtained.

The experiments [4–7] were carried out at energies below the pion photoproduction threshold. They were aimed at a more reliable determination of the electric and magnetic polarizabilities of the nucleon, $\overline{\alpha_N}$ and $\beta_N$, as compared with pioneering works [13–15]. Certain progress has been made, but room for further efforts still remains. For example, the present experimental uncertainties in the magnetic polarizability even prevent one from determining for sure the sign of $\beta_p$.

Even larger are uncertainties in the neutron polarizability $\overline{\alpha_n}$ as constrained via quasifree $\gamma n$ scattering [4]. The most precise value for the neutron electric polarizability was reported from measurements of the neutron transmission cross section of $^{208}$Pb [16]. However, the high accuracy of the announced result has been questioned [17], so that a further study of quasifree $\gamma n$ scattering would be a promising way to determine independently $\overline{\alpha_n}$ and $\beta_n$.

It is very interesting that the experimental values found for the polarizabilities of the nucleon are in severe disagreement with predictions of the naive quark model [18,19] and indicate large effects of the pion cloud [18,20], thus reviving old models of the nucleon structure [21,22]. However, quantitative estimates of the pion contribution found in the frameworks of dispersion calculations [23–25], the chiral bag model [18], the chiral perturbation theory [26,27], and soliton models [20,28,29] are very different and even contradictory. Until now an explanation of the nucleon (more generally, hadron) polarizabilities remains to be a challenge for models of hadrons [30].

In the last years, measurements of the differential cross section $d\sigma/d\Omega(\gamma p \to \gamma p)$ [8–11] and the asymmetry $\Sigma(\vec{\gamma} p \to \gamma p)$ [9] were performed in the energy region of the $\Delta$ resonance. This has led to a very accurate determination of the $M1$ photocoupling of the $\Delta$ [11], which is about 3% less than adopted in the contemporary analysis of the resonance photocouplings [31]. Such measurements have also a potential to constraint the ratio of the electric quadrupole and magnetic dipole amplitudes of $\Delta$ photoexcitation [32] (for recent theoretical work see [33] and references therein), which mainly was investigated through pion photoproduction with unpolarized and linearly polarized photons [34].

At energies above the $\Delta$ region, up to 1 GeV, the Erevan group [12] recently reported on first measurements of the beam asymmetry $\Sigma(\vec{\gamma} p \to \gamma p)$ with linearly polarized photons and concluded that none of the existing theoretical approaches describes the asymmetry at all energies. In principle, available [12,35–41] and expected experimental differential cross sections and polarization observables in $\gamma N$ scattering at energies above the $\Delta(1232)$-resonance region render it possible to carry out a multipole analysis of the data and to study mechanisms of $\gamma N$ scattering at intermediate energies. Such data provide additional information on the radiative widths of higher nucleon resonances [37,39] and can be used to find those parameters of $t$-channel exchanges in Compton scattering which are unknown presently. The latter are mainly coupling constants or, in the regime of high energies, residues of Regge poles [23].

To briefly characterize the status of available theories of elastic photon scattering on the nucleon, we may note that predictions of $s$-channel dispersion relations ([42,43] and an improved version described in the present paper) agree with all of the most exact data at energies up to 0.4 GeV (see recent discussions in [2,7,8] and, for $\gamma n$ scattering, in [4,44]). There are also other successful schemes of using dispersion relations for explaining proton Compton scattering in the first resonance region [45–48]. They use a differ-

*Electronic address: lvov@sgi.lpi.msk.su
†Electronic address: petrun@sgi.lpi.msk.su
‡Electronic address: schumacher@up200.dnet.gwdg.de

 

ent technique to treat $t$-channel exchanges (through a subtraction at fixed $u$).

In all these applications the dispersion relations use photoproduction amplitudes taken from other experiments and thus do not directly refer to fundamental parameters of hadron physics (like $\Lambda_{\rm QCD}$) or hadron models (like the quark-core radius in the chiral bag model) [49]. Nevertheless, even in this role the dispersion theory turns out to be something more than a numerical instrument for giving precise numerical predictions. Because of its ability to find separate contributions of different intermediate states, the dispersion theory clearly reveals mechanisms (or degrees of freedom) which dominate photon scattering. In the first resonance region the latter were found to be nucleon and $\Delta$ exchanges in the $s$ and $u$ channels, a rather visible contribution of nonresonant excitation of the nucleon to the $s$-wave $\pi N$ state, and $t$-channel exchanges with $\pi^0$ and effective $\sigma$ (two pion) mesons. Following these findings, successful phenomenological models incorporating these degrees of freedom can be easily constructed. Examples of such models are described in Refs. [50–53].

Much less is reliably known about mechanisms of Compton scattering at higher energies, and accurate dispersion calculations would be of great help. The only reported calculation in the second resonance region [36] which is based on dispersion relations with a subtraction at $u=m^2$ ($m$ is the nucleon mass) works rather well at c.m. angles $\theta\lesssim 90°$. It fails (as was claimed in [37]) at backward angles. The details of the calculation of Ref. [36] are not completely specified, especially those concerning the adjustment of contributions from the unphysical region, and it is not clear why this calculation gave so unrealistic results at lower energies, especially for the asymmetry $\Sigma$ and the proton polarization $\mathcal{P}$.

Less precise alternative approaches were also tried. One of those is a phenomenological resonance model [37,39]. It represents the scattering amplitude as a sum of Breit-Wigner nucleon resonances and an adjusted real background which is assumed to be a modified Born term. We will expose its results in the following discussion.

A more ambitious and deep approach to the description of Compton scattering in the resonance region uses the constituent quark model which includes all appropriate resonance states and no continuum [3]. Its great advantage is that it contains only a few parameters. The predictions of this model are very instructive, but unfortunately are too qualitative to be directly compared with experimental data on differential cross sections.

In the present paper the dispersion approach of [23,42], which is based on relativistic $s$-channel dispersion relations at finite energies for six independent invariant amplitudes of photon scattering, is extended to energies up to $E_\gamma\sim 1$ GeV. In calculating the imaginary part of the Compton scattering amplitude, we include all known mechanisms leading to large photoabsorption cross sections at these energies. We use the experimentally available photopion amplitudes of the reaction $\gamma N\to\pi N$ and inelastic contributions of well-known $\pi N$ resonances. We construct a model to include the less well-known nonresonance contributions to photoabsorption. We also construct a simple model to include $t$-channel exchanges which formally appear through the so-called asymptotic contributions. We believe that we have identified all the essential degrees of freedom, since with essentially one free parameter (the $\sigma$-meson ''mass'') we are able to satisfactorily describe all the data on proton Compton scattering at $E_\gamma\lesssim 1$ GeV, including the data on the beam asymmetry $\Sigma$ and proton polarization $\mathcal{P}$.

In the following parts of this paper we describe the formalism we use and confront its results with experimental data. Lengthy technical details are described in appendixes.

## II. DISPERSION RELATIONS AND THEIR SATURATION

Assuming Lorentz, gauge, and $P$, $T$ invariance, the general amplitude $T_{fi}$ of elastic scattering $\gamma(k)N(p)\to\gamma(k')N(p')$ at arbitrary spin projections is characterized by six cross-even invariant amplitudes $A_i$ which depend on the laboratory energy $E_\gamma$ and c.m. scattering angle $\theta$, or on the invariant variables $\nu$ and $t$, where

$$\nu=\frac{s-u}{4m}=E_\gamma+\frac{t}{4m},\quad t=(k-k')^2,\quad s=(k+p)^2,$$
$$u=(k-p')^2, \tag{1}$$

and $s+u+t=2m^2$. These amplitudes can be constructed to have no kinematic singularities and constraints and to obey the usual dispersion relations. The differential cross section

$$\frac{d\sigma}{d\Omega}=\frac{1}{64\pi^2 s}\sum_{\rm spins}|T_{fi}|^2 \tag{2}$$

and other observables (asymmetry $\Sigma$ and proton polarization $\mathcal{P}$) in terms of the amplitudes $A_i$ are specified in Appendix A.

We formulate fixed-$t$ dispersion relations for $A_i(\nu,t)$ by using a Cauchy loop of finite size (a closed semicircle of radius $\nu_{\rm max}$), so that [23,42]

$$\mathrm{Re}\,A_i(\nu,t)=A_i^{\rm pole}(\nu,t)+A_i^{\rm int}(\nu,t)+A_i^{\rm as}(\nu,t), \tag{3}$$

with

$$A_i^{\rm pole}(\nu,t)=\frac{a_i(t)}{\nu^2-t^2/16m^2},$$

$$A_i^{\rm int}(\nu,t)=\frac{2}{\pi}P\int_{\nu_{\rm thr}(t)}^{\nu_{\rm max}(t)}\mathrm{Im}A_i(\nu',t)\,\frac{\nu'd\nu'}{\nu'^2-\nu^2}. \tag{4}$$

The first term in Eq. (3) represents a singular contribution due to the nucleon in the intermediate state. It is completely determined by the electric charge and magnetic moment of the nucleon (see Appendix A).

We label the second term in Eq. (3) as the integral contribution. This is the usual dispersion integral taken, however, in between the pion photoproduction threshold, $\nu_{\rm thr}(t)=E_{\rm thr}+t/4m$ with $E_{\rm thr}\simeq 150$ MeV, to the maximum energy $\nu_{\rm max}$, below which the imaginary part can be evaluated from unitarity and known amplitudes of meson photoproduction. In our calculations we will use $E_{\rm max}=\nu_{\rm max}(t)-t/4m=1.5$ GeV.

The contribution of higher energies is represented by the last term, the so-called asymptotic contribution $A_i^{\rm as}(\nu,t)$. We discuss $A_i^{\rm int}$ and $A_i^{\rm as}$ in the following two subsections.

### A. Integral contributions

The integral contributions $A_i^{\rm int}$ are determined by the imaginary part of the Compton scattering amplitude which is given by the unitarity relation of the generic form

$$2\,{\rm Im}T_{fi}=\sum_n\,(2\pi)^4\delta^4(P_n-P_i)T_{nf}^*T_{ni}\,. \tag{5}$$

In Appendix B details are specified as for taking into account the intermediate states $n=\pi N$. In those formulas we insert the pion photoproduction multipoles $E_{l\pm}$, $M_{l\pm}$ from a recent analysis of the VPI group [31], viz., variant SM95, up to and including the angular momentum $j_{\rm max}=7/2$, and take higher partial waves in the one-pion-exchange (OPE) approximation. We introduce a small 2.8% reduction of the resonance strength of $\Delta$ photoexcitation (see Appendix B) as compared with that read out from the VPI-SM95 solution. This more correct resonance strength of $\Delta$ was recently established by the Mainz experiments on Compton scattering in the $\Delta$ region [11], and is already incorporated in the very recent version of the VPI multipoles (the solution SP96K of April 1996, the code SAID [31]).

Instead of summing up the partial-wave series $\Sigma_{j=j_{\rm max}+1}^{\infty}$ with the OPE amplitudes $T_{ni}$, we have evaluated analytically the total contribution $\Sigma_{j=1/2}^{\infty}$ of the OPE diagram to Im $T_{fi}$ (see Appendix C) and then subtracted the contribution $\Sigma_{j=1/2}^{j_{\rm max}}$ of the lowest OPE partial waves by using Eq. (B11). Such a procedure makes the partial-wave series better convergent at high $t$.

In fact, the OPE amplitude is a part of the total Born amplitude of the reaction $\gamma N\to\pi^{\pm}N$ which includes $s$-, $u$-, and $t$-channel exchanges [54]. Taken alone, the $t$-channel contribution (C1) is not gauge invariant. Therefore, it would be meaningful to use the Born amplitude rather than its OPE part (C1). This, however, makes no difference because we consider via the OPE approximation only multipoles with high $j$. In the gauge $e_\mu p^\mu=0$ we use, where $p^\mu$ is the momentum of the initial nucleon, the Born amplitude of $\gamma p\to\pi^+ n$ differs from the OPE amplitude by the $s$-channel contribution which contains only $s$ and $p$ waves with total angular momentum $j=1/2$ [54]. In the case of other reactions $\gamma n\to\pi^- p$ or $\gamma N\to\pi^0 N$, the Born amplitude does differ from the OPE approximation in all partial waves, but this difference is very small at all energies considered when $j$ is as large as 7/2. In general, the OPE approximation is very appropriate to treat partial waves with high angular momentum.

The contributions with high angular momenta, when evaluated analytically, do not result in a pathological behavior of Im$A_i(\nu',t)$ in the unphysical region of very small (near-threshold) $\nu'$ and very high $-t$ which corresponds to an unphysical cosine of the photon scattering angle $-z'\gg1$ (such kinematics arises in the integrand when we consider photon scattering at high energies and backward angles). This, however, may not be the case when partial waves with high $j$ are taken approximately from experimental fits and then multiplied by appropriate polynomials of high power in $z'$. To partly resolve this problem, we used as an experimental input to the integrand at low energies 150–400 MeV only the $j\leqslant3/2$ waves, and used the theoretical OPE values for higher multipoles. This is quite sufficient for high-quality representation of the photoproduction amplitudes at energies up to 400 MeV. At higher energies all the waves up to $j=7/2$ were taken, as they are, from the VPI analysis. Such a procedure enabled us to stabilize numerical predictions of the dispersion calculations up to backward angles and energies $E_\gamma\lesssim1$ GeV. At higher energies the contribution of $d$ waves from small $\nu'$ introduces uncertainties in the very far extrapolation to large unphysical cosines $z'$ and destroys stability of the predictions. We checked that the cutoff of the $d$ waves at energies below $\sim$400 MeV was not necessary for our purposes because it did not change to any essential extent the calculated amplitudes at energies $\sim$1 GeV. Physically, it is very improbable that small amplitudes in the near-threshold excitation of the nucleon play any role when scattering at $\sim$1 GeV is considered, and their cutoff does not seem unreasonable. Nevertheless, in general, divergences in the partial-wave expansions at low $\nu'$ make it difficult to get reliable predictions of the fixed-$t$ dispersion relations at $-t\gtrsim1$ GeV$^2$, and other approaches (like perturbative QCD) might work there better.

In the energy range considered here, photoproduction of pion pairs becomes very essential for a correct evaluation of Im$A_i$ and, therefore of the integral contributions $A_i^{\rm int}$. We used the following procedure consisting of four steps.

(1) Rescaling of the resonance contributions of $\pi N$ to Im $A_i$ to include inelastic decays of the $\pi N$ resonances. The resonance couplings were taken from the VPI analysis SM95 [31]. We also introduced a correction for a different phase space of two-pion decays of the resonances (see Appendix D).

The other steps (2), (3), and (4) are necessary to take into account the nonresonant mechanisms of photoproduction.

(2) Calculation of the imaginary parts due to intermediate $\pi\Delta$ states by using the amplitudes of the quasi-two-body reaction [55]

$$\gamma N\to\pi\Delta \tag{6}$$

in the one-pion-exchange approximation. This approximation accurately takes into account pionic states with ''high'' angular momenta $L\geqslant L_{\rm min}$, provided the second pion correlates with the nucleon to form the $\Delta$. In practice, however, we took as they are all the contributions of the OPE diagram of Eq. (6) [56,57] starting from $L_{\rm min}=1$. We calculated again, in an analytical form, an exact contribution of the whole diagram to Im $A_i$ and kept the $L=0$ part to be changed afterwards [in the step (4)]. Then a cutoff $\Lambda=0.5$ GeV in the momentum transfer was applied to the whole OPE contribution to emphasize its peripheral part and to ensure a decrease of the OPE cross section of Eq. (6) at energies $E_\gamma>1$ GeV, in accordance with experimental data. Detailed are given in Appendix E.

(3) Another mechanism which might lead to high angular momenta is the diffraction one. We assume that photoproduction of $\rho^0$ mesons at $E_\gamma>1$ GeV [55] is of diffractive origin and obeys $s$-channel helicity conservation [58]. This

assumption enables us to disentangle contributions of the reaction $\gamma N \to \rho^0 N$ to the different helicity amplitudes $\mathrm{Im}T_{fi}$ and to find all $\mathrm{Im}A_i$ (see Appendix F).

(4) After isolation, during the previous steps, of the mechanisms which are able to produce peripheral states with ''high'' angular momentum, we assume that all the rest $\Delta\sigma$ of the photoabsorption cross section includes only short-range states which are mainly excited through $E1$ transitions at the energies considered. The cross section $\Delta\sigma$ is found as a difference of the smoothed experimental total photoabsorption cross section [59,60] and the cross sections found during the steps (1)–(3). We attribute to those rest states the angular momentum $j=3/2$ (rather then $j=1/2$) both because of statistical weight and since there is a prominent contact Kroll-Ruderman-like diagram in the reaction (6) generating $\pi\Delta$ mainly in the $s$ wave, at least when the $\Delta$ is not relativistic. Then individual contributions to $\mathrm{Im}\,A_i$ can be determined (for details see Appendix G). We can partly change the quantum numbers of these states [e.g., by assuming that 30% of $\Delta\sigma$ is caused by the $E1(j=1/2)$] and see the changes in the results of the computations. Generally, they are not too large, but do favor the $E1(j=3/2)$ ansatz.

Schematically, we may write steps (1)–(4) as an equation

$$\sigma_{\mathrm{tot}} = \sigma_{\pi N} + \sigma_{N^* \to \pi\pi N,\, \eta N, \ldots} + \sigma_{\pi\Delta\text{-nonres}} + \sigma_{\rho^0 N} + \Delta\sigma_{E1(j=3/2)}, \tag{7}$$

used to calculate the $s$-channel absorptive parts of the amplitudes $A_i$ at energies up to 1.5 GeV.

### B. Asymptotic contributions

To evaluate the asymptotic contributions in Eq. (3), we have to consider high-energy behavior of the amplitudes $A_i$. Using (i) the standard assumption of a power behavior $\sim \nu^{\alpha(t)}$ of the helicity amplitudes $T_{\lambda_1'\lambda_2',\lambda_1\lambda_2}$ at fixed $t$ and $\nu \to \infty$ with the Regge pole trajectory $\alpha(t) \lesssim 1$ in the physical region and (ii) relations of the helicity amplitudes $T_{\lambda_1'\lambda_2',\lambda_1\lambda_2}$ with the amplitudes $A_i$ (see in Appendix B), we find the amplitudes $A_i$ to be

$$A_{1,2} \sim \nu^{\alpha(t)}, \quad A_{3,5,6} \sim \nu^{\alpha(t)-2}, \quad \text{and} \quad A_4 \sim \nu^{\alpha(t)-3} \quad \text{at} \quad \nu \to \infty. \tag{8}$$

Thus, the amplitudes $A_{3,4,5,6}$ vanish when $\nu \to \infty$ and hence satisfy unsubtracted dispersion relations. Therefore, the asymptotic contributions for these amplitudes are given by the dispersion integrals taken over the energies $\nu > \nu_{\max}$:

$$A_i^{\mathrm{as}}(\nu,t) = \frac{2}{\pi} \int_{\nu_{\max}(t)}^{\infty} \mathrm{Im}A_i(\nu',t)\, \frac{\nu' d\nu'}{\nu'^2 - \nu^2} \quad (i = 3,4,5,6). \tag{9}$$

In contrast, the two other amplitudes $A_1$ and $A_2$ do not vanish at high $\nu$ and the corresponding asymptotic contributions cannot be determined through $\mathrm{Im}A_i$, i.e., in terms of photoproduction. Their estimates should be based on different physical input, for example, on the Regge pole model which can describe the amplitudes in the complex energy plane at high $\nu$. Using a Cauchy loop of finite size, we can recast the asymptotic contributions $A_{1,2}^{\mathrm{as}}$ to an integral over the upper semicircle:

$$A_i^{\mathrm{as}}(\nu,t) = \frac{1}{\pi}\, \mathrm{Im} \int_{\nu' = \nu_{\max}(t) e^{i\phi},\ 0<\phi<\pi} A_i(\nu',t)\, \frac{\nu' d\nu'}{\nu'^2 - \nu^2}. \tag{10}$$

In fact, this form is valid for any of the amplitudes $A_i$. Being equivalent to Eq. (9) for $i=3,4,5,6$, it is obligatory only for $A_{1,2}$. Both Eq. (9) and Eq. (10) imply that the energy dependence of the asymptotic contributions $A_i^{\mathrm{as}}(\nu,t)$ can be neglected provided $\nu^2 \ll \nu_{\max}^2$. Accordingly, in the following we will consider the asymptotic contributions as functions of $t$ only.

We expect that the asymptotic contributions $A_{3,4,5,6}^{\mathrm{as}}$ are small, i.e., that the convergent dispersion integrals (3) and (9) for the amplitudes $A_{3,4,5,6}$, are saturated by low energies $\nu' \ll \nu_{\max}$. One can get an exact estimate in the particular case of forward Compton scattering by using the optical theorem which reads in terms of the amplitudes $A_i$ like

$$\sigma_{\mathrm{tot}}(\nu) = -2\nu\, \mathrm{Im}[A_3(\nu,0) + A_6(\nu,0)] \equiv -2\nu\, \mathrm{Im}A_{3+6}(\nu,0). \tag{11}$$

Using the data [59,60] for the total photoabsorption cross section $\sigma_{\mathrm{tot}}$, we find that the asymptotic part of $A_{3+6}$ with $\nu_{\max} = 1.5$ GeV contributes only 6% to the sum of the electric and magnetic polarizabilities of the nucleon as given by the Baldin-Lapidus sum rule:

$$\overline{\alpha_N} + \overline{\beta_N} = \frac{1}{2\pi^2} \int_{\nu_{\mathrm{thr}}}^{\infty} \sigma_{\mathrm{tot}}(\nu)\, \frac{d\nu}{\nu^2} = -\frac{1}{2\pi} A_{3+6}^{\text{non-Born}}(0,0) = -\frac{1}{2\pi} [A_{3+6}^{\mathrm{int}}(0,0) + A_{3+6}^{\mathrm{as}}(0,0)] \simeq 14 \times 10^{-4}\ \mathrm{fm}^3 \quad \text{for the proton.} \tag{12}$$

Among the small asymptotic pieces $A_{3,4,5,6}^{\mathrm{as}}(t)$ the largest one is expected to be $A_6^{\mathrm{as}}(t)$. This expectation is motivated by the approximate helicity independence of Compton scattering [61] or related photoproduction of vector mesons at high energies [58]: Only the amplitude $\mathrm{Im}A_6(\nu',t)$ gets a contribution of the leading order $O(\nu'^{\alpha(t)-2})$ from the largest (helicity-non-flip) amplitudes $T_{\pm 1\,1/2,\pm 1\,1/2}(\nu',t)$ (see Appendix B). Nowadays the helicity independence of high-energy Compton scattering is questioned because of a visible violation of the Gerasimov-Drell-Hearn sum rule (see [62,63] and references therein). If so, the amplitude $\mathrm{Im}\,A_4(\nu',t)$ in Eq. (9) may also be not quite negligible at energies $\nu' \gtrsim 1.5$ GeV and contribute through $A_4^{\mathrm{as}}$ to the differential cross section of Compton scattering at low energies only few times less than the amplitude $A_6$ does. However, this is still marginal for our present calculations since the asymptotic contribution $A_6^{\mathrm{as}}$ itself is rather small. For these reasons we keep only $A_6^{\mathrm{as}}$ and not $A_4^{\mathrm{as}}$ or $A_{3,5}^{\mathrm{as}}$.

The optical theorem unambiguously determines the asymptotic contribution $A_6^{\mathrm{as}} \simeq A_{3+6}^{\mathrm{as}}$ at zero angle. As for the $t$ dependence of $A_6^{\mathrm{as}}(t)$, we suppose that it is given by $\exp(Bt/2)$ with $B \simeq 6\ \mathrm{GeV}^{-2}$, i.e., that it follows the $t$ dependence of

the differential cross section of proton Compton scattering in the few-GeV energy region [64]. Again, the exact form of this $t$ dependence is marginal for our consideration.

Much more important are asymptotic contributions to the amplitudes $A_{1,2}$ which do not satisfy *unsubtracted* dispersion relations. Both amplitudes $A_{1,2}$ are related to photon helicity-flip transitions without and with nucleon helicity flip, respectively. They are coefficients of the Lorentz-invariant structures $F_{\mu\nu}F^{*\prime\mu\nu}\overline{u'}u$ and $i\epsilon_{\mu\nu\alpha\beta}F^{\mu\nu}F^{*\prime\alpha\beta}\overline{u'}\gamma_5 u$ in the scattering amplitude (here $F_{\mu\nu}=k_\mu e_\nu-k_\nu e_\mu$, $F'_{\mu\nu}=k'_\mu e'_\nu-k'_\nu e'_\mu$ are the electromagnetic fields of initial and final photons, and $u,u'$ are the nucleon bispinors) and get contributions from scalar and pseudoscalar $t$-channel exchanges with $J^{PC}=0^{++}$ and $0^{-+}$, respectively. At high energies such amplitudes are not well known from experiment or theory, although some constraints can be obtained (see in [23,42]). To practically treat this situation, in the present work we prefer to try and confront with experimental data a simple saturation by $t$-channel resonances of the asymptotic contributions to $A_{1,2}$.

Note that the integral contributions $A_i^{\rm int}$ in Eq. (3) cannot have pole singularities in $t$ because $\mathrm{Im}\,A_i(\nu',t)$ do not have them. For example, with a finite number of partial waves of photoproduction amplitudes used to evaluate these imaginary parts, the latter become polynomials in cosine of the scattering angle and, hence, in $t$. Therefore, whenever the amplitudes $A_{1,2}$ have a pole in $t$ related to a $t$-channel exchange by a stable particle, such a pole can enter to the right-hand side (RHS) of Eq. (3) only through the asymptotic contribution. Referring for a more refined discussion to Refs. [23,42], where the $\nu_{\max}$ dependence is also considered, we can give here a simplified explanation which is directly relevant to the $\pi^0$ exchange. In the physical region of negative $t$ the Regge trajectory of the pion is $\alpha_\pi(t)<0$ and $\alpha_\pi(0)\simeq-0.02$. Therefore, the exchange by $\pi^0$ and its numerous partners lying at the same Regge trajectory gives the contribution to the cross-even amplitude $A_2$,

$$A_2(\nu',t)\propto \nu'^{\,\alpha_\pi(t)}+(-\nu')^{\alpha_\pi(t)} =\{1+\exp[-i\pi\alpha_\pi(t)]\}\,\nu'^{\,\alpha_\pi(t)}, \tag{13}$$

which vanishes at infinity and does not prevent us from using the unsubtracted dispersion relation for $A_2$. Therefore, one can certainly represent the asymptotic $\pi^0$ contribution to the amplitude $A_2$ in the form (9). However, according to Eq. (13), the imaginary part of $A_2(\nu',t)$ considered as a function of $\nu'$ has a tail $\mathrm{Im}\,A_2(\nu',t)=C(t)\nu'^{\,\alpha_\pi(t)}$ which is very long whenever $\alpha_\pi(t)$ is a small negative number. If the coupling $C(t)$ does not vanish, the corresponding integral of this tail,

$$\int_{\nu_{\max}}^{\infty}\nu'^{\,\alpha_\pi(t)}\,\frac{d\nu'}{\nu'}=-\frac{1}{\alpha_\pi(t)}\,\nu_{\max}^{\alpha_\pi(t)}, \tag{14}$$

develops a $\pi^0$-exchange pole when extrapolated to the point $t=m_\pi^2$ in which $\alpha_\pi(t)=0$. At negative $t$ the pole is absent, but the integrand still retains the long tail which is not taken into account through the integral (4) taken over low energies $\nu'\leqslant\nu_{\max}$. We may state that the asymptotic contributions in Eq. (3) are related to the nearest $t$-channel pole exchanges (more generally, $t$-channel singularities), and the latter provide a convenient way to handle the tails in the imaginary parts.

Accordingly, we assume here that the asymptotic contributions $A_{1,2}^{\rm as}$ are nothing but the contributions of $t$-channel exchanges with the lightest scalar and pseudoscalar particles. They are $\sigma$ and $\pi^0$ mesons, where $\sigma$, as usual, is an effective particle representing a correlated pion pair (note, however, that there is growing evidence that the $\sigma$ can be more than an effective particle [65–67]). Our assumption is in line with the experimental fact [58,61] that the dominating Regge-pole exchange with the highest $\alpha(t)$ entering into Eq. (8) (i.e., Pomeron) has very small couplings in helicity-flip vertices and, therefore, may be less important at low energies of $\nu\lesssim1.5$ GeV than the exchanges with lower $\alpha(t)$, such as $\pi^0$ and $\sigma$.

Thus, we use the Low amplitude of the $\pi^0$ exchange as the substitute for the asymptotic contribution to $A_2$:

$$A_2^{\rm as}(t)\simeq A_2^{\pi^0}(t)=\frac{g_{\pi NN}F_{\pi^0\gamma\gamma}}{t-m_{\pi^0}^2}\,\tau_3F_\pi(t), \tag{15}$$

where the isospin factor is $\tau_3=\pm1$ for the proton and neutron, respectively, and the product of the $\pi NN$ and $\pi^0\gamma\gamma$ couplings is

$$g_{\pi NN}F_{\pi^0\gamma\gamma}=-16\pi\sqrt{\frac{g_{\pi NN}^2}{4\pi}\frac{\Gamma_{\pi^0\to2\gamma}}{m_{\pi^0}^3}} =(-0.331\pm0.012)\ \ \mathrm{GeV}^{-1}, \tag{16}$$

provided $g_{\pi NN}^2/4\pi=13.75\pm0.15$ [68] and $\Gamma_{\pi^0\to2\gamma}=7.74\pm0.55$ eV [69]. The minus sign in Eq. (16) is chosen in accordance with the sign of the axial anomaly contribution (see [70]). In the chiral limit the $\pi^0\gamma\gamma$ coupling follows from the Wess-Zumino-Witten effective chiral Lagrangian [71] and thus

$$g_{\pi NN}F_{\pi^0\gamma\gamma}=g_A\,\frac{m}{f_\pi}\left(-\frac{e^2N_c}{12\pi^2f_\pi}\right)=-0.321\ \ \mathrm{GeV}^{-1} \tag{17}$$

(with $g_A=1.2573\pm0.0028$, $f_\pi=92.4\pm0.3$ MeV [69], and $N_c=3$), in remarkable agreement with the experimental number (16). We insert in Eq. (15) an off-shell form factor $F_\pi(t)$, which stems from $\pi NN$ and $\pi^0\gamma\gamma$ vertices, and take it in the monopole form, $F_\pi(t)=(\Lambda_\pi^2-m_\pi^2)/(\Lambda_\pi^2-t)$ with the cutoff parameter $\Lambda_\pi=0.7$ GeV estimated from the axial radius of the nucleon and the size of the pion [72]. Its specific choice is less important than a choice of the $\sigma$-meson ''mass'' below, and, for example, with $\Lambda_\pi=1$ GeV the numerical results for the differential cross section of Compton scattering are very similar to those obtained with the $\sigma$-meson ''mass'' increased by $\sim$20 MeV.

In case of the $\sigma$ exchange we use a simpler form

$$A_1^{\rm as}(t)\simeq A_1^{\sigma}(t)=\frac{g_{\sigma NN}F_{\sigma\gamma\gamma}}{t-m_\sigma^2}. \tag{18}$$

We do not include here any form factor because at moderate $t$ its influence cannot be distinguished from the form (18) with a smaller $m_\sigma$. As we will see, phenomenologically

$m_\sigma \simeq 600$ MeV works rather successfully. To pin down the coupling constants in Eq. (18), we use the relation of the amplitude $A_1$ with the polarizabilities [76]

$$A_1^{\text{non-Born}}(0,0) = A_1^{\text{int}}(0,0) + A_1^{\text{as}}(0,0) = -2\pi(\overline{\alpha_N} - \overline{\beta_N}), \tag{19}$$

where

$$\overline{\alpha_p} - \overline{\beta_p} \simeq (10 \pm 2) \times 10^{-4} \ \text{fm}^3 \tag{20}$$

is a world average [7] over recent proton experiments. In this way the polarizabilities constrain the asymptotic contribution $A_1^{\text{as}}$ at $t=0$, whereas the parameter $m_\sigma^2$ determines the slope of $A_1^{\text{as}}(t)$ and, what is most important, the scale of $A_1^{\text{as}}(t)$ at high $-t$. We may mention that the exponential form of $A_1^{\text{as}} \sim \exp(Bt/2)$ with $B \simeq 6$ GeV$^{-2}$ used in [42] in applications to lower energies results in a too strong suppression of $A_1$ at high $t$ and, correspondingly, in a too low cross section at backward angles in the dip region between the first and second resonances.

One should not consider Eq. (18) as an assumption of an existence of a stable particle $\sigma$ giving the $t$-channel contribution of a pole form. Equation (18) rather is a monopole parametrization of the function $A_1^{\text{as}}(t)$ at negative $t, -t \lesssim 1$ GeV$^2$. Moreover, since any mechanism of $t$-channel exchange involves vertex form factors, the effective parameter $m_\sigma$ in Eq. (18) provides a lower bound for the mass of a real particle (if any), resulting in the effective exchange amplitude (18).

Although the $\sigma$ exchange used here is considered as an effective one, it is interesting that the coupling constants of the $\sigma$, which are needed to get the magnitude of the phenomenologically introduced contribution (18) and evaluated from the proton data (20) and the previously calculated $A_1^{\text{int}}(0,0)$, i.e.,

$$-\frac{1}{2\pi}[A_1^{\text{as}}(0)]_p \equiv (\overline{\alpha_p} - \overline{\beta_p})^{\text{as}} = \frac{g_{\sigma NN} F_{\sigma\gamma\gamma}}{2\pi m_\sigma^2} \simeq (12 \pm 3) \times 10^{-4} \ \text{fm}^3, \tag{21}$$

are not unrealistic [73]. In fact, they perfectly correspond to the couplings of the $\sigma$ particle in the pion-nucleon linear $\sigma$ model. In the chiral limit (i.e., $m_\pi^2 \ll m^2, m_\sigma^2$) the $\sigma$ exchange in this model gives the contribution

$$(\overline{\alpha_N} - \overline{\beta_N})^{(\sigma)} = \frac{e^2 m}{96\pi^3 m_\pi^2 f_\pi^2} = 13.4 \times 10^{-4} \ \text{fm}^3, \tag{22}$$

where the parameter $f_\pi = 92.4$ MeV determines both $\sigma\gamma\gamma$ (to one loop) and $\sigma NN$ couplings (cf. [74,75]). We cannot, however, claim that the $\sigma$ model *explains* the asymptotic contribution $A_1^{\text{as}}$ because, in the framework of this model, the term of order $O(m_\pi^{-2})$ in the amplitude $A_1$ vanishes at $\nu \to \infty$ and $A_1^{\text{as}}$ is finite in the chiral limit; cf. [24]. A realistic estimate of the asymptotic contribution might be carried out by using data on the asymmetry $\Sigma$ at high energies, similar to [23,76], or on the base of dispersion relations at backward angles [25,77].

Presently, the origin of the large contribution (21) to $\overline{\alpha_N} - \overline{\beta_N}$ is not understood. Recent calculations [25] based on available information about the $t$-channel reactions $\gamma\gamma \to \pi\pi$ and $\pi\pi \to NN$, though giving a correct sign of the contribution, reveal problems in reproducing its huge magnitude. A similar situation is seen in refined calculations in the framework of chiral perturbation theory [78], although it is masked there by rather uncertain counterterms. This is, probably, a very interesting point for further investigations. On the experimental side, studies of the distribution of the ''hidden'' polarizability (21) over the nucleon would be very helpful and desirable. It can be achieved by measuring the $t$ dependence of the Compton scattering cross sections in appropriate kinematics (see below), and by using polarized photons since the beam asymmetry $\Sigma$ is very sensitive to the amplitude $A_1$, especially at high energies [23]. Also, the use of virtual photons [79] has a great potential in discovering the space structure of the ''hidden'' polarizability (21).

## III. RESULTS AND DISCUSSION

Now we compare the predictions of the described dispersion approach to the data [8–12,35–41,80–85] on proton Compton scattering in the first and second resonance regions. We pay most attention to high energies, beyond the $\Delta$ region, where dispersion predictions were not available (except a restricted consideration in [36]). The situation at lower energies was considered rather completely elsewhere [1,2,7,8], and the present improvements introduce no essential changes there and keep the overall good agreement between the theory and experiments.

Our predictions depend on quite a number of physical quantities and a few additional parameters, such as radiative widths of nucleon resonances, the $\sigma$-meson ''mass,'' the cutoff $\Lambda$ in the OPE contribution of the reaction $\gamma N \to \pi\Delta$, etc. We did not try to fit all these quantities (partly because many data from different experiments contradict each other). Instead, we found that a reasonable agreement with the data can be achieved when the $\gamma N \to \pi N$ multipoles and the resonance parameters of the VPI group [31] were used, provided the $\sigma$-meson ''mass'' was chosen to be about 600 MeV. This is demonstrated by the solid lines in Figs. 1–6, showing the energy and angular dependence of the differential cross section, the asymmetry $\Sigma$, and the proton polarization $\mathcal{P}$. For the ''mass'' of $\sigma$ much higher than 600 MeV the asymptotic contribution $A_1^{\text{as}}(t)$ becomes a less steep function of $t$ and contributes more at backward angles, thus leading to a too high differential cross section in the energy range between the first and the second resonances (see dashed lines in Fig. 1). Choosing a larger cutoff parameter $\Lambda$ in the OPE contribution of the reaction (6), one could diminish the differential cross section and hence reduce the contradiction between the data and theoretical variants with high $m_\sigma$. However, when $\Lambda > 0.5$ GeV, the cross section of the reaction $\gamma N \to \pi\Delta$ turns out to be unreasonably large. At smaller $m_\sigma$ the differential cross section in between the resonances becomes too small. With the presently available experimental data one can exclude $m_\sigma$ less than $\simeq 400$ MeV and more than $\simeq 700$ MeV.

To describe the Erevan data for the asymmetry $\Sigma$, it is also better to choose $m_\sigma \lesssim 600$ MeV [see Fig. 3(b)]. This indication is rather important because the theoretical predictions for $\Sigma$ are not sensitive to $\Lambda$. There is a general agreement of the present calculations with the Erevan data, al-

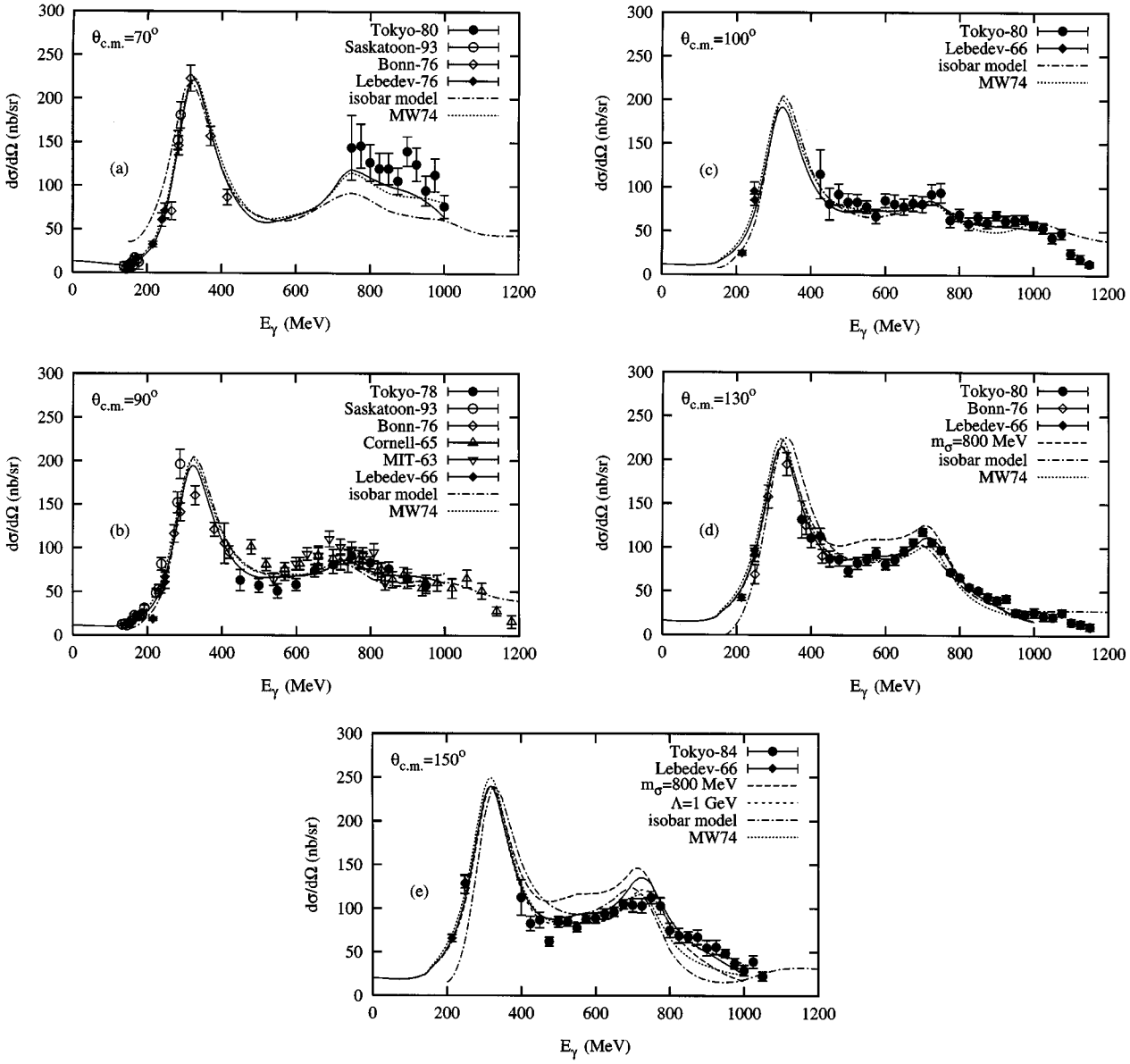


FIG. 1. Energy dependences of the c.m. differential cross section of $\gamma p$ scattering at several angles. Solid lines: the main variant (see in the text). Dashed lines: $m_\sigma$ is increased from 600 to 800 MeV. Short-dashed lines: the cutoff parameter $\Lambda$ of the OPE-$\Delta$ contribution is increased from 0.5 to 1 GeV. Dotted lines: prediction of the present approach based on the old photo pion amplitudes [86]. Predictions of the isobar model are taken from its version [37]. Data are from [8,36–41,80–85].

though the predicted asymmetry is not high enough at angles $\theta<120°$ and energies in the $D_{13}$ region (700–800 MeV). Available data on the proton polarization $\mathcal{P}$ [35,38] are in agreement with the theory as well (see Fig. 4). However, they are not precise enough to put any strict constraints to the parameters involved.

We could change our ansatz for the ''$s$-wave'' part $\Delta\sigma$ of double-pion photoproduction as being of purely $(E1,\ j=3/2)$ type. If we attribute 30% of the cross section $\Delta\sigma$ to the $(E1,\ j=1/2)$ strength (see Appendix G), the differential cross section gets a maximal change of about $-9\%$ at $E_\gamma\simeq 550$ MeV and backward angles which could be compensated by the $\sim$80 MeV increase in $m_\sigma$. However, with such parameters the asymmetry $\Sigma$ gets a negative shift of $\approx -0.1$ at energies $\gtrsim$ 800 MeV and central angles, which is not favored by the Erevan data which are described best by the $(E1,\ j=3/2)$ ansatz.

In Figs. 1–4 we also show results calculated from the older and now obsolete photopion multipoles and resonance photocouplings of [86], simply to check whether recent improvements in knowing the resonance couplings are crucial for getting an agreement with the Compton scattering data. A difference is seen mostly at energies $>$700–800 MeV and is more distinct in the asymmetry $\Sigma$ than in the differential cross section. In general, the results of dispersion calculations are sensitive to the strengths of the nucleon resonances $P_{33}(1232)$, $D_{15}(1520)$, $D_{33}(1670)$, $P_{15}(1680)$, $F_{15}(1680)$, and some others, as is illustrated in Fig. 5 where different curves are obtained by a small (10%) variation of the resonance strengths $A^r$ of the Breit-Wigner term, Eq. (D1), contributing to one- and two-pion photoproduction amplitudes. This was demonstrated before in frames of the Tokyo resonance model [37,39] where these strengths were fitted and extracted from proton Compton scattering data.

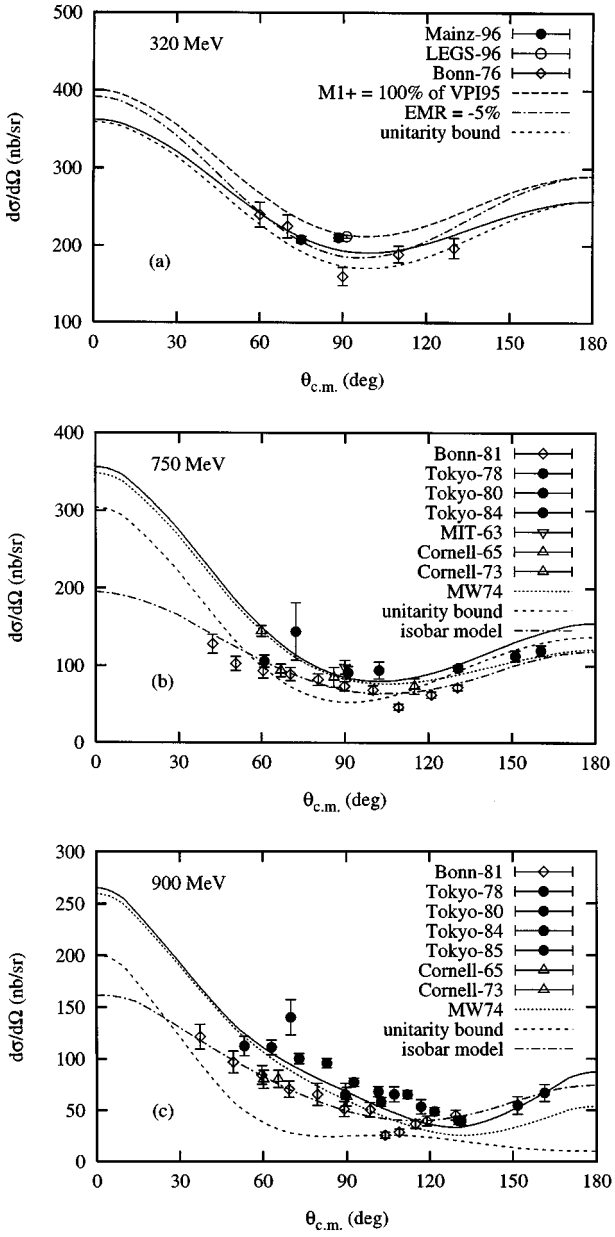


FIG. 2. Angular dependences of the c.m. differential cross section. Unitarity bounds (i.e. contributions to the cross section from Im $T_{fi}$ only) are shown by short-dashed lines. The other notation is as in Fig. 1. Data at 320 MeV include those of [9–11]. Dash-dotted lines in cases of $E=750$ and 900 MeV: the isobar model in the version of [39], i.e., with adjusted relative phases of different resonances and background.

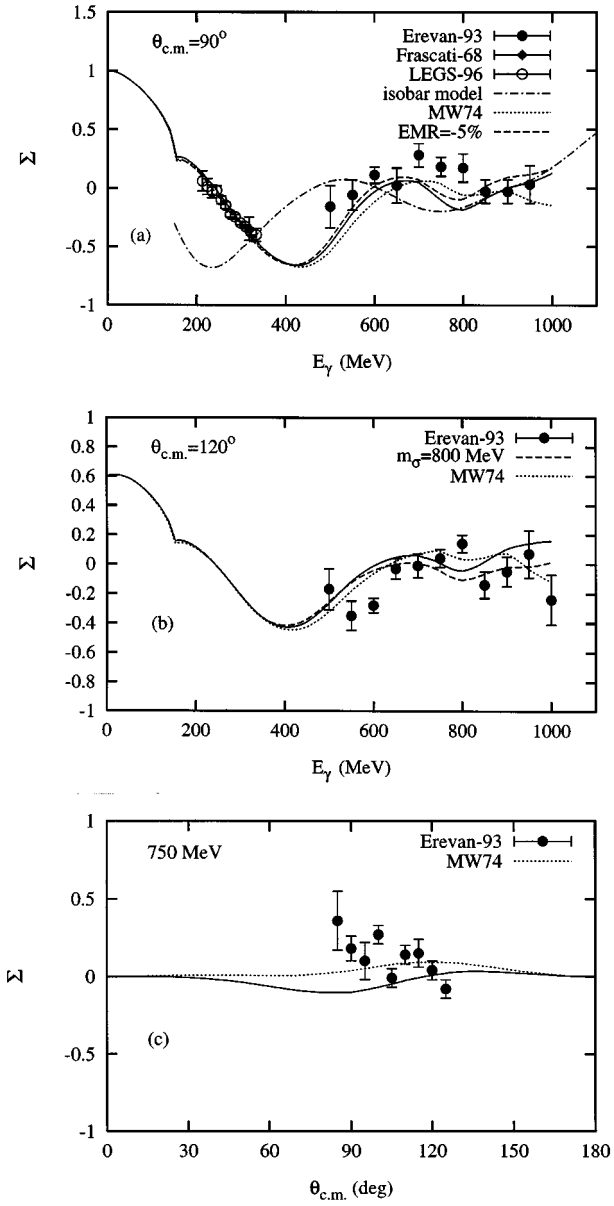


FIG. 3. Beam asymmetry in the reaction $\vec{\gamma}p\to\gamma p$ with linearly polarized photons. Notation of curves is as in Fig. 1. Data are from [9,12,83].

In the case of the $P_{33}(1232)$ resonance, its excitation amplitude becomes very well constrained by the dispersion theory and recent data on Compton scattering in the $\Lambda$ region [9–11]. Splitting the physical photopion amplitudes $M_{1+},E_{1+}$ into the $\Delta$-resonance parts $M^r_{1+},E^r_{1+}$ and a background (see Appendix D for the explicit form and energy dependence of the resonance parts used), we can rescale the resonance parts, keeping the background fixed, and thus find the physical amplitudes $M_{1+},E_{1+}$ modified in the vicinity of the resonance. In this way we calculate $M_{1+},E_{1+}$ and the corresponding Im $A_i$ and Re $A_i$ at different $M1$ and $E2$ photocouplings of the $\Delta$ resonance. We are aware of the fact that the ansatz of a fixed background does not respect the Watson theorem and therefore is not completely satisfactory, especially for $E_{1+}$ having a relatively large background part. Nevertheless, we expect that this inconsistency is not very important for fine-tuning the resonance parameters.

The best fit of the Mainz data [10,11] at the fixed ratio of the $\Delta$-resonance photocouplings,

$$\mathrm{EMR}=E^r_{1+}/M^r_{1+}=-1.6\%, \tag{23}$$

as inferred from [31], gives the resonance strength for the $M1$ excitation of the $\Delta$ slightly smaller, by $-2.8\pm0.9\%$ (including both statistical and systematic errors), than that found in the SM95 solution by the VPI group [31] (see Fig. 6). Systematic uncertainties of these data are not shown in the figure and, therefore, the agreement between the theory and the data at 90° is better than the figure suggests.

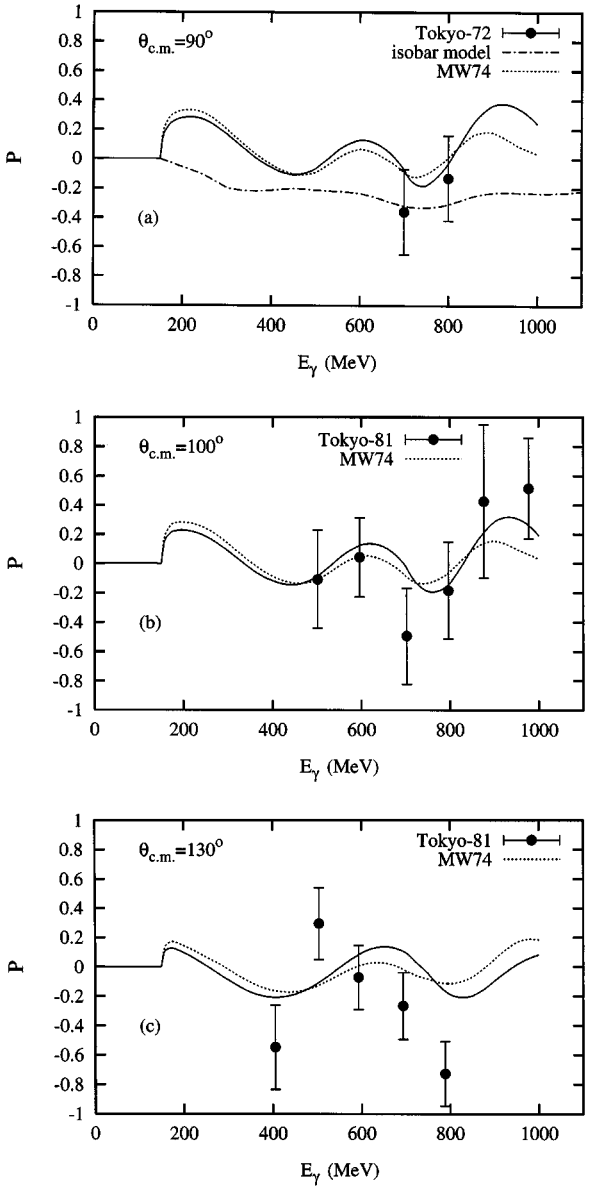


FIG. 4. Proton polarization. Notation of curves is as in Fig. 1. Data are from [35,38].

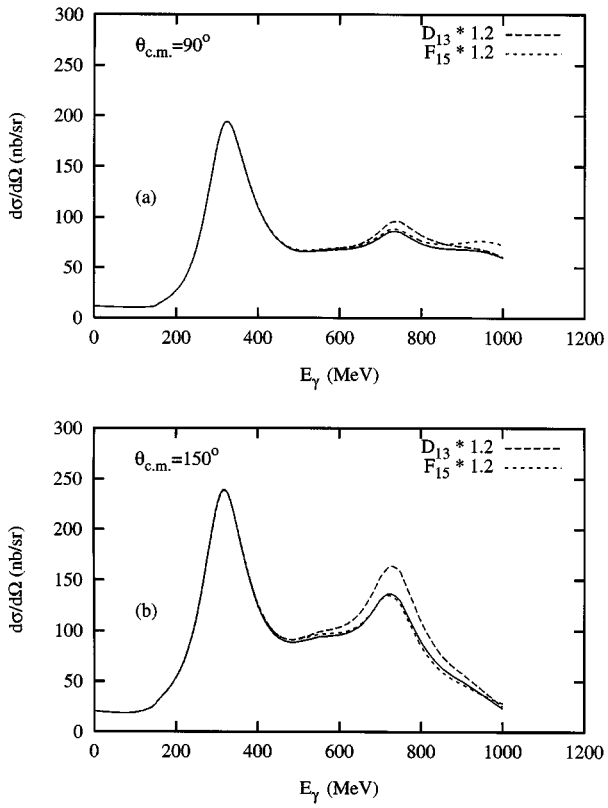


FIG. 5. Differential cross sections versus energy. The main variant (solid line) is compared with variants where the radiative widths of the $D_{13}(1520)$ (dashed line) and $F_{15}(1680)$ (dotted line) resonances are increased by 20%.

The $M1$ strength found from Compton scattering is in very good agreement with the data on the total photoabsorption cross section near the $\Delta$ peak [60]. Note that precise knowledge of $M1$ excitation of the $\Delta$ is certainly needed to reliably study smaller photoproduction multipoles in the resonance region. With more data at forward and backward angles information on the $E2$ strength of $\Delta$ photoexcitation can be inferred too. For illustration we give in Figs. 2(a) and 3(a) predictions obtained with the quadrupole amplitude $E^{r}_{1+}$ rescaled to EMR$=-5\%$.

Although the presented results of the dispersion calculations seem to be very similar to those found in the Tokyo resonance model [37,39], the nonresonant parts of the Compton scattering amplitude are very different in the two approaches. They are real and have the form of the Born term times a form factor [87] in Ref. [37] and are complex in the present approach, getting a sizable imaginary contribution from the nonresonant part of the total photoabsorption cross section (see in Fig. 7). At forward angles and energies $E_\gamma > 600$ MeV the differential cross section found in the present work through unitarity and dispersion relations is essentially higher than that in the resonance model [37,39] [see Figs. 2(b) and 2(c)], and so we believe that the latter model is inapplicable there. Estimating the success of the isobar model, one should remember that the parameters used in [37] and in [39] for the description of different kinematic regions were different too [cf. Fig. 1(e)].

We did not observe a strong sensitivity of the differential cross section, of the asymmetry $\Sigma$, or the polarization $\mathcal{P}$ to the $P_{11}(1470)$ (Roper) and $S_{11}(1535)$ resonances, in contrast to findings of [37,88]. Probably, in part this difference is related to the large amount of nonresonance contributions to the scattering amplitude we have in our approach. In our calculations we take the total photoabsorption cross section as a fixed experimental input. Therefore, at forward angles our results are not very sensitive to model-dependent details and parameters, and only at $\theta \geqslant 90°$ the predictions get a model dependence. Correspondingly, this is the most interesting region for comparison with experiments.

In conclusion, we presented a dispersion calculation of the $\gamma p$-scattering amplitude at energies over the first and second resonance regions which was based on experimental information about single-pion photoproduction and reasonable hypotheses concerning the dynamics of double-pion photoproduction and high-energy behavior of the helicity-flip amplitudes $A_{1,2}$. Comparing with the older attempt [36], we achieved a much better agreement with available data including polarization observables. One may expect that the

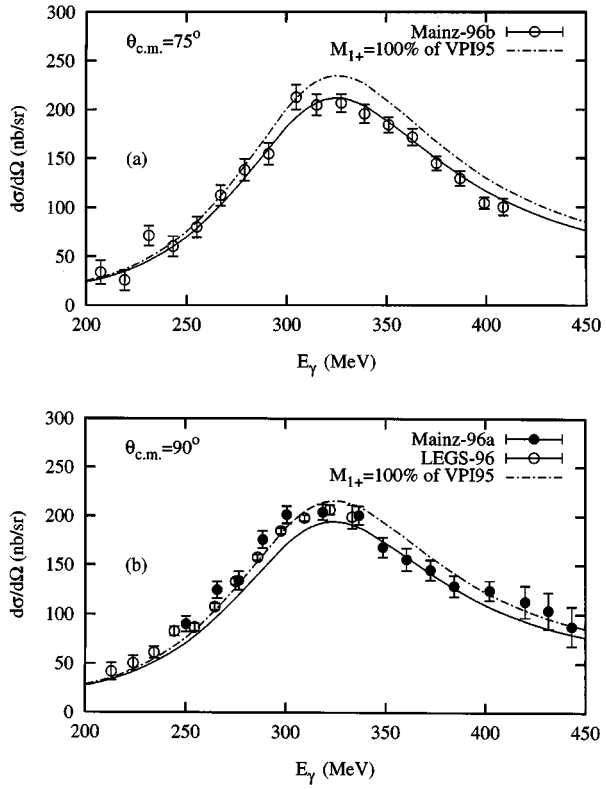


FIG. 6. Differential cross section in the Δ region. The main variant (see text) is represented by solid lines, the same but without a 2.8% reduction of the $M1$ strength of the Δ-resonance photoexcitation by the dash-dotted lines. The experimental data are from [9–11]. The exact value of the EMR ratio is of minor influence on the differential cross section at these scattering angles and has been assumed to be $-1.6\%$, just as in [31].

approach developed here can be used to get quantitative information on the resonance photocouplings, the partial-wave structure of inclusive double-pion photoproduction, and the asymptotic behavior of spin-dependent Compton amplitudes, provided more precise experimental data are available. The latter subject is the most intriguing one because it cannot be investigated in photoproduction experiments, except for the special case of forward scattering. New accurate measurements of the differential cross section $d\sigma/d\Omega$ and asymmetry $\Sigma$ at energies above 1 GeV which are feasible at CEBAF could shed more light on the role of the $t$-channel exchanges in the amplitudes $A_i(\nu,t)$. The dip region between the Δ and $D_{13}$ peaks is another promising place to study the $A_1$ amplitude and the related $\sigma$ exchange. Accurate data on the differential cross section $d\sigma/d\Omega$ and asymmetry $\Sigma$ are highly desirable there. They could help to reveal the nature of the ''hidden'' polarizability of the nucleon (21). New data in the dip region are expected from the LARA experiment carried out in Mainz [89].

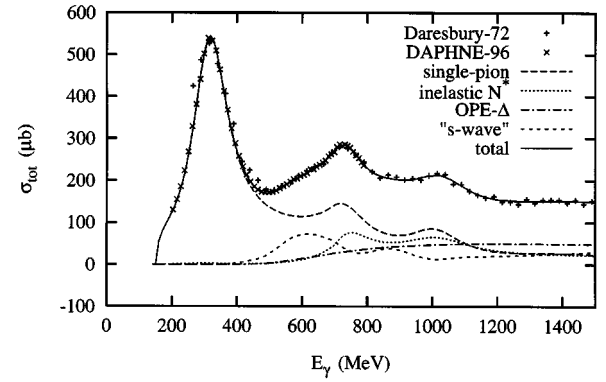


FIG. 7. Total photoabsorption cross section on the proton and its components. Dashed line: $\pi N$ channel. Dotted line: inelastic resonance contribution. Dash-dotted line: OPE contribution of $\gamma N\to\pi\Delta$. Short-dashed line: $s$-wave correction. Data are from [59,60].

Our results suggest a dominance of $\pi$ and $\sigma$ exchanges in the $t$ channel and an equally important role of both resonant and nonresonant (like $\pi\Delta$) contributions in the $s$ and $u$ channels in the region of the second resonance. This qualitative guidance may be valuable for improving dynamical models [50–53] of nucleon Compton scattering, which successfully work in the Δ region, and extending them to higher energies.

## ACKNOWLEDGMENTS

We are pleased to thank A. M. Nathan for valuable discussions. Hospitality extended by II. Physikalisches Institut der Universität Göttingen to A.L. and V.P. and by Institut für Kernphysik der Universität Mainz to A.L., where a part of work was done, is highly appreciated. This investigation was supported by Deutsche Forschungsgemeinschaft (Grants Nos. Schu-222, 438 113/173, and SFB 201) and the Russian Foundation for Basic Research (Grant No. 94-02-06555).

## APPENDIX A: INVARIANT AMPLITUDES

To describe the Compton scattering amplitude of $\gamma(k)N(p)\to\gamma'(k')N(p')$,

$$\langle f|S-1|i\rangle = i(2\pi)^4\delta^4(k+p-k'-p')T_{fi}, \qquad \text{(A1)}$$

we use the orthogonal basis suggested by Prange [90]:

$$T_{fi}=\overline{u'}(p')e'^{*\mu}\Big[-\frac{P'_\mu P'_\nu}{P'^2}(T_1+\gamma\cdot KT_2) - \frac{N_\mu N_\nu}{N^2}(T_3+\gamma\cdot KT_4)+i\frac{P'_\mu N_\nu - P'_\nu N_\mu}{P'^2K^2}\gamma_5 T_5 + i\frac{P'_\mu N_\nu + P'_\nu N_\mu}{P'^2K^2}\gamma_5\gamma\cdot KT_6\Big]e^\nu u(p). \qquad \text{(A2)}$$

Here $e$ and $e'$ are photon polarization vectors, and $u$ and $u'$ are bispinors of the nucleon normalized like $\overline{uu}=2m$, $m$ being the nucleon mass. The vectors $P'$, $K$, and $N$ together with the vector $Q$ are defined as to give four orthogonal vectors:

$$P'_\mu = P_\mu - K_\mu\frac{P\cdot K}{K^2}, \quad P=\tfrac{1}{2}(p+p'), \quad K=\tfrac{1}{2}(k'+k),$$

$$N_\mu=\epsilon_{\mu\alpha\beta\gamma}P'^\alpha Q^\beta K^\gamma, \quad Q=\tfrac{1}{2}(p-p')=\tfrac{1}{2}(k'-k), \qquad \text{(A3)}$$

where $\epsilon_{\mu\alpha\beta\gamma}$ is an antisymmetric tensor and $\epsilon_{0123}=1$; also $\gamma_5=\left(\begin{smallmatrix}0 & 1\\ 1 & 0\end{smallmatrix}\right)$.

The six amplitudes $T_i$ introduced are analytical functions of energy and scattering angle with the only singularities related to one-particle exchanges and inelastic thresholds in the $s$, $u$, and $t$ channels [91,92]. As a result of crossing symmetry, the amplitudes $T_2(\nu,t)$ and $T_4(\nu,t)$ are odd functions of $\nu$; the other four amplitudes are even functions.

It is convenient to introduce linear combinations of the amplitudes $T_i$ which are free from kinematic constraints [93]. Such constraints arise because the denominators in the kinematic structures in Eq. (A2) vanish at forward and backward angles like

$$K^2=-\frac{t}{4}=\frac{1}{8s}(s-m^2)^2(1-\cos\theta),$$

$$P'^2K^2=\frac{1}{4}(su-m^4)=-\frac{1}{8s}(s-m^2)^2(1+\cos\theta),$$

$$N^2=P'^2(K^2)^2\sim\sin^2\theta. \tag{A4}$$

These linear combinations are [42]

$$A_1=\frac{1}{t}[T_1+T_3+\nu(T_2+T_4)]=-\frac{1}{2}A_1^{\rm BT},$$

$$A_2=\frac{1}{t}[2T_5+\nu(T_2+T_4)]=\frac{m}{2}A_2^{\rm BT},$$

$$A_3=\frac{m^2}{m^4-su}\left[T_1-T_3-\frac{t}{4\nu}(T_2-T_4)\right]$$
$$=-\frac{m^2}{4}A_5^{\rm BT}-\frac{m^2}{4\nu}A_6^{\rm BT},$$

$$A_4=\frac{m^2}{m^4-su}\left[2mT_6-\frac{t}{4\nu}(T_2-T_4)\right]=-\frac{m^2}{4\nu}A_6^{\rm BT},$$

$$A_5=\frac{1}{4\nu}[T_2+T_4]=\frac{m}{2\nu}A_3^{\rm BT},$$

$$A_6=\frac{1}{4\nu}[T_2-T_4]=-\frac{m}{2}A_4^{\rm BT}+\frac{4m^2-t}{16\nu}A_6^{\rm BT}, \tag{A5}$$

where we also give their relations with similar invariant amplitudes $A_i^{\rm BT}$ introduced by Bardeen and Tung [93]. The amplitudes $A_i(\nu,t)$ are even functions of $\nu$ and have no kinematic singularities or kinematic constraints.

In terms of the amplitudes $T_i$ the differential cross section in the c.m. frame is given by

$$\frac{d\sigma}{d\Omega}=\frac{1}{64\pi^2s}\{\tfrac{1}{2}(4m^2-t)(|T_1|^2+|T_3|^2)$$
$$-\tfrac{1}{2}(s-m^2)(u-m^2)(|T_2|^2+|T_4|^2)$$
$$+m(s-u)\mathrm{Re}(T_1T_2^*+T_3T_4^*)$$
$$-t|T_5|^2+(m^4-su)|T_6|^2\}. \tag{A6}$$

The beam asymmetry with linearly polarized photons is

$$\sum=\frac{d\sigma_\perp-d\sigma_\parallel}{d\sigma_\perp+d\sigma_\parallel}=\left(64\pi^2s\,\frac{d\sigma}{d\Omega}\right)^{-1}$$
$$\times\{\tfrac{1}{2}(4m^2-t)(|T_3|^2-|T_1|^2)$$
$$-\tfrac{1}{2}(s-m^2)(u-m^2)(|T_4|^2-|T_2|^2)$$
$$+m(s-u)\mathrm{Re}(T_3T_4^*-T_1T_2^*)\}, \tag{A7}$$

and polarization of recoil protons is

$$\mathcal{P}=\frac{d\sigma_y-d\sigma_{-y}}{d\sigma_y+d\sigma_{-y}}=\left(64\pi^2s\,\frac{d\sigma}{d\Omega}\right)^{-1}\frac{(s-m^2)^2}{2\sqrt{s}}$$
$$\times\sin\theta\ \mathrm{Im}(T_1^*T_2+T_3^*T_4). \tag{A8}$$

The amplitudes $A_i$ have poles at zero energy because of contributions of the nucleon in the intermediate state. These poles are contained in two Born diagrams with the pole propagator $(\gamma\cdot p-m)^{-1}$ and on-shell vertices $\Gamma_\mu(p+k,p)=\gamma_\mu+[\gamma\cdot k,\gamma_\mu]\kappa/4m$, where $\kappa=1.793q-1.913(1-q)$ is the nucleon anomalous magnetic moment. We introduced here the electric charge of the nucleon, $q=(1+\tau_3)/2=1$ or 0. The Born contributions to the amplitudes $A_i$ have a pure pole form

$$A_i^{\rm Born}(\nu,t)=A_i^{\rm pole}(\nu,t)=\frac{me^2r_i(t)}{(s-m^2)(u-m^2)}, \tag{A9}$$

where $e$ is the elementary electric charge ($e^2/4\pi\simeq1/137$) and

$$r_1=-2q+(\kappa^2+2q\kappa)\frac{t}{4m^2},$$

$$r_2=2q\kappa+2q+(\kappa^2+2q\kappa)\frac{t}{4m^2},$$

$$r_3=r_5=\kappa^2+2q\kappa,\quad r_4=\kappa^2,\quad r_6=-\kappa^2-2q\kappa-2q. \tag{A10}$$

## APPENDIX B: CONTRIBUTION OF $\pi N$ INTERMEDIATE STATES

Our procedure used to explicitly find the imaginary parts of the amplitudes $A_i$ in the $s$ channel is based on the formalism of helicity amplitudes. First we introduce six independent helicity amplitudes for Compton scattering, $T_{\lambda_1'\lambda_2',\lambda_1\lambda_2}(s,\theta,\phi)$, and define the reduced helicity amplitudes $\tau_i$ which are free from the kinematic factors of the form $[\cos(\theta/2)]^{|\lambda+\lambda'|}[\sin(\theta/2)]^{|\lambda-\lambda'|}e^{i\phi(\lambda-\lambda')}$, $\lambda=\lambda_1-\lambda_2$, $\lambda'=\lambda_1'-\lambda_2'$:

$$T_{1(1/2),1(1/2)}=\cos\frac{\theta}{2}\,\tau_1,\quad T_{-1(1/2),-1(1/2)}=\cos^3\frac{\theta}{2}\,\tau_2,$$

$$T_{1-(1/2),1(1/2)}=\cos^2\frac{\theta}{2}\sin\frac{\theta}{2}\,\tau_3,$$

$$T_{1\,(1/2),-1(1/2)}=\cos\frac{\theta}{2}\sin^2\frac{\theta}{2}\,\tau_4,$$

$$T_{-1-(1/2),1(1/2)}=\sin\frac{\theta}{2}\,\tau_5,\quad T_{1-(1/2),-1(1/2)}=\sin^3\frac{\theta}{2}\,\tau_6. \tag{B1}$$

Here $\theta$ is the c.m. scattering angle, and the scattering plane is chosen to be the azimuthal plane ($\phi=0$). Other helicity amplitudes $T_{\lambda_1'\lambda_2',\lambda_1\lambda_2}(s,\theta,\phi)$ can be found through $P$ or $T$ inversion:

$$T_{-\lambda_1'-\lambda_2',-\lambda_1-\lambda_2}=T_{\lambda_1\lambda_2,\lambda_1'\lambda_2'}=(-)^{\lambda_2-\lambda_2'}T_{\lambda_1'\lambda_2',\lambda_1\lambda_2}$$

$$\text{at } \phi=0. \tag{B2}$$

In terms of the helicity amplitudes the invariant amplitudes $A_i(s,t)$ read

$$A_1=\frac{1}{(s-m^2)^2}\left[-\frac{s}{m}\left(1-\sigma\frac{s+m^2}{2s}\right)\tau_4-\frac{\sqrt{s}}{2}(\tau_5+\sigma\tau_6)\right],$$

$$A_2=\frac{1}{(s-m^2)^3}\left[-\frac{s}{m}(s+m^2)\left(1-\sigma\frac{s-m^2}{2s}\right)\tau_4-\frac{\sqrt{s}}{2}(s-m^2)\tau_5+2s\sqrt{s}\left(1-\sigma\frac{s-m^2}{4s}\right)\tau_6\right],$$

$$A_3=\frac{1}{(s-m^2)^2(s-m^2+t/2)}\left[m^3[\tau_1+(1-\sigma)\tau_2]-2m^2\sqrt{s}\left(1-\sigma\frac{s+m^2}{2s}\right)\tau_3\right],$$

$$A_4=\frac{1}{(s-m^2)^2(s-m^2+t/2)}\left[m^3\tau_1-m^3\left(1+\sigma\frac{m^2}{s}\right)\tau_2+\frac{2m^4}{\sqrt{s}}\sigma\tau_3\right],$$

$$A_5=\frac{1}{(s-m^2)^2(s-m^2+t/2)}[m(s+m^2)\sigma\tau_4-m^2\sqrt{s}(\tau_5+\sigma\tau_6)],$$

$$A_6=\frac{1}{(s-m^2)^2(s-m^2+t/2)}\left[-\frac{m}{2}(s+m^2)[\tau_1+(1-\sigma)\tau_2]+2m^2\sqrt{s}(1-\sigma)\tau_3\right]. \tag{B3}$$

Here

$$\sigma=\sin^2\frac{\theta}{2}=-\frac{st}{(s-m^2)^2}. \tag{B4}$$

The helicity amplitudes have a standard partial-wave decomposition in terms of $d$ functions:

$$T_{\lambda_1'\lambda_2',\lambda_1\lambda_2}(s,\theta,\phi)=8\pi\sqrt{s}\sum_j(2j+1)T^j_{\lambda_1'\lambda_2',\lambda_1\lambda_2}(s)\times d^j_{\lambda\lambda'}(\theta)e^{i\phi(\lambda-\lambda')}. \tag{B5}$$

In the case of two-body intermediate states $n$ like $\pi N$, the imaginary parts of the partial waves are given by the partial waves of the reaction $\gamma N\to n$ as follows:

$$\mathrm{Im}[T^j_{\lambda_1'\lambda_2',\lambda_1\lambda_2}(s)]^{(n)}=\sum_n q[T^j_{n,\lambda_1'\lambda_2'}(s)]^*T^j_{n,\lambda_1\lambda_2}(s), \tag{B6}$$

where $q$ is the c.m. momentum of the intermediate particles and the sum is taken over helicities and other quantum numbers of these particles. Of course, different intermediate states contribute additively to the imaginary parts.

Normally partial waves for single-pion photoproduction are given in terms of multipole amplitudes with definite parity and orbital momentum $l$, $E_{l\pm}$ and $M_{l\pm}$, or those with definite $l$ and helicity, $A_{l\pm}$ and $B_{l\pm}$. They are related with the helicity partial waves in the form

$$T^{j=k+1/2}_{0(1/2),1(1/2)}=-T^{j=k+1/2}_{0-(1/2),-1-(1/2)}=\frac{i}{\sqrt{2}}(-A_{k+}-A_{(k+1)-}),$$

$$T^{j=k+(1/2)}_{0-(1/2),1(1/2)}=-T^{j=k+(1/2)}_{0\,(1/2),-1-(1/2)}=\frac{i}{\sqrt{2}}(-A_{k+}+A_{(k+1)-}),$$

$$T^{j=k+(1/2)}_{0\,(1/2),1-(1/2)}=-T^{j=k+(1/2)}_{0-(1/2),-1(1/2)}=i\sqrt{\frac{k(k+2)}{8}}(B_{k+}+B_{(k+1)-}),$$

$$T^{j=k+(1/2)}_{0-(1/2),1-(1/2)}=-T^{j=k+(1/2)}_{0\,(1/2),-1(1/2)}=i\sqrt{\frac{k(k+2)}{8}}(B_{k+}-B_{(k+1)-}). \tag{B7}$$

Also

$$A_{k+}=\frac{1}{2}[(k+2)E_{k+}+kM_{k+}],\quad B_{k+}=E_{k+}-M_{k+},$$

$$A_{(k+1)-}=\frac{1}{2}[-kE_{(k+1)-}+(k+2)M_{(k+1)-}],$$

$$B_{(k+1)-}=E_{(k+1)-}+M_{(k+1)-}. \tag{B8}$$

Using these relations and explicit representations of the $d$ functions, we may write the imaginary parts of the reduced helicity amplitudes $\tau_i$ in the form

$$\mathrm{Im}[\tau_1]^{(1\pi)}=8\pi q\sqrt{s}\sum_{k\geqslant 0}(2k+2)(|A_{k+}|^2+|A_{(k+1)-}|^2)\times F(-k,k+2,1,\sigma),$$

$$\mathrm{Im}[\tau_5]^{(1\pi)}=8\pi q\sqrt{s}\sum_{k\geqslant 0}2(k+1)^2(|A_{k+}|^2-|A_{(k+1)-}|^2)\times F(-k,k+2,2,\sigma),$$

$$\mathrm{Im}[\tau_2]^{(1\pi)}=8\pi q\sqrt{s}\sum_{k\geqslant 1}\frac{k(k+1)(k+2)}{2}\times(|B_{k+}|^2+|B_{(k+1)-}|^2)F(-k+1,k+3,1,\sigma),$$

$$\mathrm{Im}[\tau_6]^{(1\pi)}=8\pi q\sqrt{s}\sum_{k\geqslant 1}\frac{k^2(k+1)^2(k+2)^2}{12}\times(-|B_{k+}|^2+|B_{(k+1)-}|^2)F(-k+1,k+3,4,\sigma),$$

$$\mathrm{Im}[\tau_3]^{(1\pi)}=8\pi q\sqrt{s}\sum_{k\geqslant 1}k(k+1)(k+2)\times(-A_{k+}B^*_{k+}-A_{(k+1)-}B^*_{(k+1)-})\times F(-k+1,k+3,2,\sigma),$$

$$\mathrm{Im}[\tau_4]^{(1\pi)}=8\pi q\sqrt{s}\sum_{k\geqslant 1}\frac{k(k+1)^2(k+2)}{2}\times(A_{k+}B^*_{k+}-A_{(k+1)-}B^*_{(k+1)-})\times F(-k+1,k+3,3,\sigma),\qquad\text{(B9)}$$

where $q$ is the pion momentum and the sum over different isotopic channels is implied. $F$ is a hypergeometric polynomial of the $\sigma=\sin^2(\theta/2)$:

$$F(a,b,c,x)=1+\frac{ab}{c}\frac{x}{1!}+\frac{a(a+1)b(b+1)}{c(c+1)}\frac{x^2}{2!}+\cdots.\qquad\text{(B10)}$$

In our calculations we take the partial-wave amplitudes $E_{l\pm}$ and $M_{l\pm}$ with the angular momentum $j\leqslant j_{\max}=7/2$ ($j\leqslant 3/2$ below 400 MeV) from the phenomenological analysis [31] of photopion experimental data with the following except [11]. The $M_{1+}$ amplitude of the VPI group was split into the $P_{33}(1232)$-resonance part $M^r_{1+}$ specified in Appendix D and a background $M^b_{1+}$. The resonance photocouplings were taken from [31]. Then the resonance part of $M_{1+}$ was rescaled down by 2.8% and the resulting amplitude $0.972M^r_{1+}+M^b_{1+}$ was used as a new $M_{1+}$ in dispersion calculations. It has reduced $M1$ strength in the vicinity of the $\Delta$ resonance, which is necessary to be consistent with experimental data on Compton scattering and photoproduction; cf. [11].

Higher multipoles are assumed to be given by the one-pion-exchange diagram. They are

$$A_{k+}=-\frac{k}{2}f_3\beta_k+\frac{k+2}{2}f_4\beta_{k+1},\quad B_{k+}=-f_3\beta_k+f_4\beta_{k+1},$$

$$A_{(k+1)-}=\frac{k}{2}f_4\beta_k-\frac{k+2}{2}f_3\beta_{k+1},\quad B_{(k+1)-}=-f_4\beta_k+f_3\beta_{k+1},\qquad\text{(B11)}$$

where

$$f_3=\mp\frac{eg_{\pi NN}}{4\pi\sqrt{2s}}\sqrt{\frac{E_{N'}+m}{E_N+m}},$$

$$f_4=\mp\frac{eg_{\pi NN}}{4\pi\sqrt{2s}}v\sqrt{\frac{E_N+m}{E_{N'}+m}},\qquad\text{(B12)}$$

with $E_N$ and $E_{N'}$ being the c.m. energies of the initial and final nucleons, respectively, and $v$ being the c.m. velocity of the pion. The quantity $g_{\pi NN}>0$ is the $\pi NN$ coupling constant, $g^2_{\pi NN}/4\pi\simeq 13.75$, and the sign $\mp$ has to be taken for $\pi^\pm$ photoproduction. Also, $\beta_k$ are functions of $v$ and given by

$$\beta_k=\frac{1}{2k+1}[Q_{k-1}(w)-Q_{k+1}(w)],$$

$$Q_k(w)=\frac{1}{2}\int_{-1}^{1}P_k(z)\frac{dz}{w-z},\quad w=\frac{1}{v},\qquad\text{(B13)}$$

in terms of Legendre functions of the second kind.

## APPENDIX C: OPE CONTRIBUTION OF $\pi N$ INTERMEDIATE STATES

The series (B9) and (B11) can be used straightforwardly to sum up the contributions to $\mathrm{Im}\,A_i$ from the intermediate states $\pi N$ with the angular momentum $j>j_{\max}=7/2$ by using the OPE approximation. Another way to find the sum of contributions to $\mathrm{Im}\,A_i$ is to calculate the total OPE contribution to $\mathrm{Im}\,A_i$ in a closed analytical form from all partial waves and then to subtract the OPE contribution of the waves with $j\leqslant j_{\max}$ which is determined directly by Eqs. (B9). Such a procedure is especially helpful in calculations at high $t$ when the series (B9) may be divergent because of the singularity induced by the one-pion exchange. When the OPE contribution is eliminated, the convergence of the subtracted series is essentially improved.

The total OPE contribution to $\mathrm{Im}\,A_i$ is determined as follows. In the c.m. frame, the OPE amplitude of the reaction $\gamma N\to\pi^\pm N$ reads

$$\frac{1}{8\pi\sqrt{s}}T_\gamma=\frac{v\mathbf{e}\cdot\hat{\mathbf{q}}}{1-v\hat{\mathbf{k}}\cdot\hat{\mathbf{q}}}(-i\boldsymbol{\sigma}\cdot\hat{\mathbf{k}}f_3+i\boldsymbol{\sigma}\cdot\hat{\mathbf{q}}f_4),\qquad\text{(C1)}$$

where $f_3$ and $f_4$ are defined in Eqs. (B12). Therefore, the imaginary part of the Compton scattering amplitude in the OPE approximation is given by the integral

$$\frac{1}{8\pi\sqrt{s}}\,\mathrm{Im}\,T_{fi}^{\mathrm{OPE}}=\frac{q}{4\pi}\int\frac{v^2\mathbf{e}'^*\cdot\hat{\mathbf{q}}\,\mathbf{e}\cdot\hat{\mathbf{q}}\,d\Omega_q}{(1-v\hat{\mathbf{k}}'\cdot\hat{\mathbf{q}})(1-v\hat{\mathbf{k}}\cdot\hat{\mathbf{q}})}(\boldsymbol{\sigma}\cdot\hat{\mathbf{k}}'f_3-\boldsymbol{\sigma}\cdot\hat{\mathbf{q}}f_4)(\boldsymbol{\sigma}\cdot\hat{\mathbf{k}}f_3-\boldsymbol{\sigma}\cdot\hat{\mathbf{q}}f_4),\tag{C2}$$

which, in turn, is reduced to the integrals

$$\frac{1}{4\pi}\int\frac{\hat{\mathbf{q}}_i\hat{\mathbf{q}}_j d\Omega_q}{(1-v\hat{\mathbf{k}}'\cdot\hat{\mathbf{q}})(1-v\hat{\mathbf{k}}\cdot\hat{\mathbf{q}})}\equiv\alpha(v,z)\,\delta_{ij}+\beta(v,z)(\hat{\mathbf{k}}_i\hat{\mathbf{k}}_j+\hat{\mathbf{k}}'_i\hat{\mathbf{k}}'_j)+\gamma(v,z)(\hat{\mathbf{k}}_i\hat{\mathbf{k}}'_j+\hat{\mathbf{k}}'_i\hat{\mathbf{k}}_j),$$

$$\frac{1}{4\pi}\int\frac{\hat{\mathbf{q}}_i\hat{\mathbf{q}}_j\hat{\mathbf{q}}_k d\Omega_q}{(1-v\hat{\mathbf{k}}'\cdot\hat{\mathbf{q}})(1-v\hat{\mathbf{k}}\cdot\hat{\mathbf{q}})}\equiv a(v,z)(\hat{\mathbf{k}}_i\hat{\mathbf{k}}_j\hat{\mathbf{k}}_k+\hat{\mathbf{k}}'_i\hat{\mathbf{k}}'_j\hat{\mathbf{k}}'_k)+b(v,z)(\hat{\mathbf{k}}_i\hat{\mathbf{k}}_j\hat{\mathbf{k}}'_k+\hat{\mathbf{k}}_i\hat{\mathbf{k}}'_j\hat{\mathbf{k}}_k+\hat{\mathbf{k}}'_i\hat{\mathbf{k}}_j\hat{\mathbf{k}}_k+\hat{\mathbf{k}}'_i\hat{\mathbf{k}}'_j\hat{\mathbf{k}}_k+\hat{\mathbf{k}}'_i\hat{\mathbf{k}}_j\hat{\mathbf{k}}'_k+\hat{\mathbf{k}}_i\hat{\mathbf{k}}'_j\hat{\mathbf{k}}'_k)$$
$$+c(v,z)(\hat{\mathbf{k}}_i\delta_{jk}+\hat{\mathbf{k}}_j\delta_{ik}+\hat{\mathbf{k}}_k\delta_{ij}+\hat{\mathbf{k}}'_i\delta_{jk}+\hat{\mathbf{k}}'_j\delta_{ik}+\hat{\mathbf{k}}'_k\delta_{ij}),$$

$$\frac{1}{4\pi}\int\frac{\hat{\mathbf{q}}_i\hat{\mathbf{q}}_j\hat{\mathbf{q}}_k d\Omega_q}{1-v\hat{\mathbf{k}}\cdot\hat{\mathbf{q}}}\equiv A'(v)(\hat{\mathbf{k}}_i\delta_{jk}+\hat{\mathbf{k}}_j\delta_{ik}+\hat{\mathbf{k}}_k\delta_{ij})+B'(v)\hat{\mathbf{k}}_i\hat{\mathbf{k}}_j\hat{\mathbf{k}}_k.\tag{C3}$$

Here the functions $\alpha,\beta,\gamma,a,b,c,A',B'$ depend on the pion velocity $v$ and the photon scattering c.m. angle, $z=\cos\theta$. They are given, in terms of the more elementary integrals,

$$\frac{1}{4\pi}\int\frac{d\Omega_q}{(1-v\hat{\mathbf{k}}'\cdot\hat{\mathbf{q}})(1-v\hat{\mathbf{k}}\cdot\hat{\mathbf{q}})}\equiv\phi_1(v,z),$$

$$\frac{1}{4\pi}\int\frac{d\Omega_q}{1-v\hat{\mathbf{k}}\cdot\hat{\mathbf{q}}}\equiv\phi_2(v),$$

$$\frac{1}{4\pi}\int\frac{\hat{\mathbf{q}}_i d\Omega_q}{(1-v\hat{\mathbf{k}}'\cdot\hat{\mathbf{q}})(1-v\hat{\mathbf{k}}\cdot\hat{\mathbf{q}})}\equiv v\,\phi_3(v,z)(\hat{\mathbf{k}}_i+\hat{\mathbf{k}}'_i),$$

$$\frac{1}{4\pi}\int\frac{\hat{\mathbf{q}}_i d\Omega_q}{1-v\hat{\mathbf{k}}\cdot\hat{\mathbf{q}}}\equiv v\,\phi_4(v)\hat{\mathbf{k}}_i,$$

$$\frac{1}{4\pi}\int\frac{\hat{\mathbf{q}}_i\hat{\mathbf{q}}_j d\Omega_q}{1-v\hat{\mathbf{k}}\cdot\hat{\mathbf{q}}}\equiv A(v)\,\delta_{ij}+B(v)\hat{\mathbf{k}}_i\hat{\mathbf{k}}_j,\tag{C4}$$

as follows:

$$\alpha(v,z)=\phi_1(v,z)-2\phi_3(v,z),$$
$$\beta(v,z)=\phi_3(v,z)-\alpha(v,z)-z\gamma(v,z),$$

$$\gamma(v,z)=\frac{1}{1-z^2}\,[z\phi_1(v,z)+(1-3z)\phi_3(v,z)-\phi_4(v)],$$

$$c(v,z)=\frac{\alpha(v,z)-A(v)}{(1+z)v},$$

$$b(v,z)=\frac{1}{1+z}\left[\frac{1}{v}\,\gamma(v,z)-c(v,z)\right],$$

$$a(v,z)=\frac{1}{v}\,\beta(v,z)-zb(v,z)-2c(v,z),$$

$$A'(v)=\frac{1}{v}\left(A(v)-\frac{1}{3}\right),\quad B'(v)=\frac{1}{v}\,B(v)-2A'(v).\tag{C5}$$

The functions $\phi_i$ read

$$\phi_2(v)=\frac{1}{2v}\log\frac{1+v}{1-v},\quad \phi_4(v)=\frac{1}{v^2}\,(\phi_2(v)-1),$$

$$\phi_3(v,z)=\frac{\phi_1(v,z)-\phi_2(v)}{(1+z)v^2},\tag{C6}$$

and

$$\phi_1(v,z)=\frac{1}{vR}\log\frac{R+(1-z)v}{R-(1-z)v},$$

$$R=\sqrt{(1-z)[2-(1+z)v^2]}.\tag{C7}$$

Also

$$A(v)=\tfrac{1}{2}[\phi_2(v)-\phi_4(v)],\quad B(v)=\phi_4(v)-A(v).\tag{C8}$$

In terms of the integrals introduced, the imaginary part of the Compton scattering amplitude (C2) is given by the functions

$$\mathrm{Im}R_1^{\mathrm{OPE}}=qv^2\left[(\alpha+z\gamma)(zf_3^2+f_4^2)-\frac{2}{v}\,(\alpha+z\gamma-A)f_3f_4\right],$$

$$\mathrm{Im}R_2^{\mathrm{OPE}}=qv^2\gamma\left[-zf_3^2-f_4^2+\frac{2}{v}\,f_3f_4\right],$$

$$\mathrm{Im}R_3^{\mathrm{OPE}}=qv^2f_3[[z\alpha+(z^2-1)\gamma]f_3-2[(z^2-1)b+(2z-1)c]f_4],$$

$$\mathrm{Im}R_4^{\mathrm{OPE}}=qv^2f_3[\alpha f_3-2cf_4],$$

$$\mathrm{Im}R_5^{\mathrm{OPE}}=qv^2f_3[-(\alpha+z\gamma)f_3+(2zb+3c)f_4],$$

$$\mathrm{Im}R_6^{\mathrm{OPE}}=qv^2f_3[\gamma f_3-(2b+c)f_4],\tag{C9}$$

which, by definition, represents the scattering amplitude in three-dimensional notation,

$$\frac{1}{8\pi\sqrt{s}}T_{fi}=\mathbf{e}'^{*}\cdot\mathbf{e}\,R_1+\mathbf{s}'^{*}\cdot\mathbf{s}\,R_2+i\boldsymbol{\sigma}\cdot\mathbf{e}'^{*}\times\mathbf{e}\,R_3$$
$$+i\boldsymbol{\sigma}\cdot\mathbf{s}'^{*}\mathbf{s}\,R_4+i(\boldsymbol{\sigma}\cdot\hat{\mathbf{k}}\,\mathbf{s}'^{*}\cdot\mathbf{e}-\boldsymbol{\sigma}\cdot\hat{\mathbf{k}}'\,\mathbf{e}'^{*}\cdot\mathbf{s})R_5$$
$$+i(\boldsymbol{\sigma}\cdot\hat{\mathbf{k}}'\,\mathbf{s}'^{*}\cdot\mathbf{e}-\boldsymbol{\sigma}\cdot\hat{\mathbf{k}}\,\mathbf{e}'^{*}\cdot\mathbf{s})R_6 \qquad \text{(C10)}$$

(here $\mathbf{s}=\hat{\mathbf{k}}\times\mathbf{e}$, $\mathbf{s}'=\hat{\mathbf{k}}'\times\mathbf{e}'$), and gives the reduced helicity amplitudes $\tau_i$:

$$\tau_1=8\pi\sqrt{s}\left[\cos^2\frac{\theta}{2}\,(R_1+R_2-R_3-R_4+2R_5+2R_6)\right.$$
$$\left.+2R_3+2R_4\right],$$
$$\tau_2=8\pi\sqrt{s}[R_1+R_2-R_3-R_4-2R_5-2R_6],$$
$$\tau_3=8\pi\sqrt{s}[R_1+R_2-R_3-R_4],$$
$$\tau_4=8\pi\sqrt{s}[R_1-R_2-R_3+R_4],$$
$$\tau_5=8\pi\sqrt{s}\left[\sin^2\frac{\theta}{2}\,(R_1-R_2-R_3+R_4-2R_5+2R_6)\right.$$
$$\left.+2R_3-2R_4\right],$$
$$\tau_6=8\pi\sqrt{s}[R_1-R_2-R_3+R_4+2R_5-2R_6]. \qquad \text{(C11)}$$

The above formulas for $\mathrm{Im}\,R_i^{\mathrm{OPE}}$, together with relations of $R_i$ with $\tau_i$ and $A_i$, just determine the total OPE contribution to the imaginary part of the Compton scattering amplitude.

## APPENDIX D: RESONANCE CONTRIBUTION OF $\pi\pi N$ INTERMEDIATE STATES

Considering resonance contributions to imaginary parts of the Compton scattering amplitudes, we start with Walker's parametrization of the amplitudes of resonance photoexcitation [54,86]:

$$A^{\mathrm{res}}(W)=A^r\sqrt{\frac{k_0q_0}{kq}}\,\frac{W_0\sqrt{\Gamma_\gamma\Gamma_\pi}}{W_0^2-W^2-iW_0\Gamma}, \qquad \text{(D1)}$$

where $A^{\mathrm{res}}$ is the resonance part of any of the amplitudes $A_{l\pm}, B_{l\pm}$ of the reaction $\gamma N\to\pi N$, the widths with bars

$$\overline{\Gamma}_\pi(W)=\Gamma_0\left(\frac{q}{q_0}\right)^{2l+1}\left(\frac{q_0^2+X^2}{q^2+X^2}\right)^{l},$$
$$\overline{\Gamma}_\gamma(W)=\Gamma_0\left(\frac{k}{k_0}\right)^{2j_\gamma}\left(\frac{k_0^2+X^2}{k^2+X^2}\right)^{j_\gamma} \qquad \text{(D2)}$$

are energy-dependent pionic and radiative widths, respectively, normalized to the total width $\Gamma_0$ at the peak, and the total width $\Gamma(W)$ is taken to be equal to $\overline{\Gamma}_\pi(W)$. Also $k$ and $q$ are photon and pion momenta in the channels $\gamma N$ and $\pi N$ at the energy $W=\sqrt{s}$, and $k_0$ and $q_0$ are the same quantities at the resonance energy $W=W_0$. Photon and pion angular momenta $j_\gamma$ and $l$, together with the parameters $X$, determine barrier penetration factors. We take all of them from [86], except $j_\gamma$. Since the VPI group parametrizes the radiative widths by using $j_\gamma=1$ [94], we do so here too.

For the amplitudes $A^r$ of the resonance multipoles at the resonance energies we use recent results of the VPI group [31], as well as their resonance masses $W_0$ and widths $\Gamma_0$.

Being used in Eqs. (B9), the resonance multipoles (D1) determine contributions $[\mathrm{Im}\tau_i]^{(N^*\to\pi N)}$ of single-pion decays of nucleon resonances to imaginary parts of the Compton scattering amplitudes. To determine the contributions of the resonance decays to other channels (mostly $\pi\pi N$), we assume the validity of the Breit-Wigner formula and rescale the $\pi N$ contribution with the factor

$$R=\frac{1-B_\pi}{B_\pi}\,\frac{\overline{\Gamma}_{\mathrm{inel}}(W)}{\overline{\Gamma}_\pi(W)}, \qquad \text{(D3)}$$

where $\overline{\Gamma}_{\mathrm{inel}}(W)$ is the normalized width of the decays $N^*\to(\pi\pi N,\eta N,\pi\pi\pi N,\ldots)$ and $B_\pi$ is the single-pion branching ratio of the resonance $N^*$ which pins down $\Gamma_{\mathrm{inel}}(W_0)$. We take $B_\pi$ from [31] as well.

For the energy dependences of the inelastic widths $\overline{\Gamma}_{\mathrm{inel}}$ we generally use the ansatz

$$\overline{\Gamma}_{\mathrm{inel}}(W)=\Gamma_0\left(\frac{Q}{Q_0}\right)^{2l+4}\left(\frac{Q_0^2+X^2}{Q^2+X^2}\right)^{l+2}, \qquad \text{(D4)}$$

where $Q$ is the momentum of a compound particle $(2\pi)$ with the mass $2m_\pi$ in the channel $(2\pi)N$, and $Q_0=Q(W=W_0)$. Such an ansatz takes into account the correct energy behavior $\sim(W-2m_\pi-m)^2$ of the phase space near the three-body threshold and also incorporates a barrier penetration factor similar to that in Eqs. (D2).

We make two exceptions from Eq. (D4):

(i) For the $P_{33}(1232)$ resonance its inelastic branching ratio $1-B_\pi\simeq0.6\%$ is related to the radiative decay $\Delta\to\gamma N$. Accordingly, we use $\overline{\Gamma}_{\mathrm{inel}}(W)=\overline{\Gamma}_\gamma(W)$ in this case.

(ii) For the $S_{11}(1535)$ resonance its inelastic decay is mainly due to $\eta N$ mode, and in this case we use $\overline{\Gamma}_{\mathrm{inel}}(W)=\Gamma_0 q_\eta(W)/q_\eta(W_0)$, where $q_\eta$ is the c.m. momentum of $\eta$. In particular, using the parameters from [31], we get the cross section of $\sigma_{\gamma p\to S_{11}\to\eta p}\simeq12\ \mu$b at the resonance peak which is close to the experimentally known magnitude [95,96] given by $2\xi^2q_\eta/k\simeq13$ to 15 $\mu$b in terms of the quantity $\xi$ introduced in [96].

To maintain unitarity, we also replace in Eq. (D1) Walker's total width by

$$\Gamma=B_\pi\overline{\Gamma}_\pi+(1-B_\pi)\overline{\Gamma}_{\mathrm{inel}}. \qquad \text{(D5)}$$

Thus, our procedure to calculate inelastic contributions of $\pi N$ resonances to $\mathrm{Im}\tau_i$ is given by

$$[\mathrm{Im}\tau_i]^{(N^*\to\pi\pi N\ldots)}=R\{[\mathrm{Im}\tau_i]^{(N^*\to\pi N)}\}_{\Gamma\to\text{Eq. (D5)}} \qquad \text{(D6)}$$

(for each resonance $N^*$). In Fig. 7 we show the resonance total cross section of $\gamma N\to N^*\to\pi\pi N$... (dotted line) which is easily found from $\mathrm{Im}\tau_i$ through optical theorem, i.e., $\mathrm{Im}(\tau_1+\tau_5)(\nu,0^\circ)=4m\nu\sigma_{\mathrm{tot}}(\nu)$.

## APPENDIX E: OPE CONTRIBUTION OF $\pi\Delta$ INTERMEDIATE STATES

The model we use to split the nonresonance part of the $\gamma N\to\pi\pi N$ cross section into individual multipoles is based on the assumption that all partial waves except the lowest one are dominated by the mechanism of one-pion exchange in the reaction $\gamma N\to\pi\Delta$. Here we give details of how to calculate the related imaginary part of the Compton scattering amplitude.

The effective Lagrangian of the $\pi N\Delta$ transition in the Rarita-Schwinger formalism reads

$$L=\frac{G}{m_\pi}\,\overline{\psi_\mu}T\psi\partial^\mu\pi+\text{H.c.}, \tag{E1}$$

where $T$ is the transition isospin operator normalized to Clebsch-Gordan coefficients. The coupling $G$ determines the decay width of the $\Delta$:

$$\Gamma=\frac{E'+m}{12\pi M}\,\frac{G^2q'^3}{m_\pi^2},\quad \frac{G^2}{4\pi}=0.38, \tag{E2}$$

where $M$ is the mass of the $\Delta$, and $E'$ and $q'$ are energy and momentum of the final nucleon in the decay $\Delta\to\pi' N$.

We write the OPE amplitude of $\gamma(k)N(p)\to\pi(q)\Delta(P)$ as

$$T=-i\,\frac{eG}{m_\pi}\,\overline{u_\mu}(P)u(p)\,\frac{e\cdot q}{k\cdot q}. \tag{E3}$$

We do all the calculations in the c.m. frame and use the three-dimensional gauge $e_0=0$ in which the diagrams supplementing the OPE diagram to a complete gauge-invariant set are suppressed or have a dominating $s$-wave component which will be adjusted separately in the following. Using the amplitude (E3) in the unitarity relation, we find the imaginary part of the Compton scattering amplitude:

$$\frac{1}{8\pi\sqrt{s}}\,[\mathrm{Im}T]^{\text{OPE-}\Delta}=-\frac{4}{3}\,q\,\frac{e^2G^2}{64\pi^2sm_\pi^2}\int\frac{d\Omega_q}{4\pi}\,\frac{e\cdot qe'\cdot q}{k\cdot qk'\cdot q}\,\overline{u'}(p')\Big\{\gamma\cdot P\Big[p\cdot p'+\frac{m^2}{3}+\frac{m}{3M}\,(p\cdot P+p'\cdot P)$$
$$-\frac{2}{3M^2}\,p\cdot Pp'\cdot P\Big]+M\Big[p\cdot p'-\frac{m^2}{3}-\frac{m}{3M}\,(p\cdot P+p'\cdot P)-\frac{4}{3M^2}\,p\cdot Pp'\cdot P\Big]\Big\}u(p). \tag{E4}$$

Here the term in curly brackets stems from the $\Delta$ propagator and the factor of 4/3 appears after summing over the $\pi^-\Delta^{++}$ and $\pi^+\Delta^0$ channels.

In three-dimensional notation the RHS of Eq. (E4) is recast as

$$C\int\frac{d\Omega_q}{4\pi}\,\frac{\mathbf{e}\cdot\hat{\mathbf{q}}\,\mathbf{e}'\cdot\hat{\mathbf{q}}}{ZZ'}\Big\{\Big[P_1+\frac{y}{2}\,(1-2d)(Z+Z')-y^2ZZ'\Big]\Big[P_2+\frac{y}{2}\,(Z+Z')+\frac{vy}{2}\,i\boldsymbol{\sigma}\cdot(\hat{\mathbf{k}}-\hat{\mathbf{k}}')\times\hat{\mathbf{q}}+if_1\boldsymbol{\sigma}\cdot\hat{\mathbf{k}}'\times\hat{\mathbf{k}}\Big]$$
$$+\Big[P_3-\frac{y}{2}\,(1+4d)(Z+Z')-2y^2ZZ'\Big]\cdot(P_4-if_2\boldsymbol{\sigma}\cdot\hat{\mathbf{k}}'\times\hat{\mathbf{k}})\Big\}. \tag{E5}$$

Here

$$f_1=\frac{P_0(p_0-m)}{2mM},\quad f_2=\frac{p_0-m}{2m},$$

$$y=\frac{\omega q_0}{mM},\quad d=\frac{M^2+m^2-m_\pi^2}{2mM},$$

$$Z=1-v\hat{\mathbf{k}}\cdot\hat{\mathbf{q}},\quad Z'=1-v\hat{\mathbf{k}}'\cdot\hat{\mathbf{q}},$$

$$P_1=2+d-d^2+\frac{3\omega^2}{2m^2}\,(1-z),$$

$$P_3=1-d-2d^2+\frac{3\omega^2}{2m^2}\,(1-z),$$

$$P_2=d-f_1(1-z),\quad P_4=1+f_2(1-z),$$

$$C=-\frac{16m^3Mqv^2}{9\omega^2}\left(\frac{eG}{8\pi\sqrt{s}}\right)^2,\quad v=\frac{q}{q_0}, \tag{E6}$$

and $\omega$, $p_0,q_0,P_0$ are the energies of $\gamma$, $N$, $\pi$, $\Delta$. The angular integral in Eq. (E5) is calculated with the use of formulas from Appendix C. In terms of the amplitudes $R_i$ and functions $A,\alpha,\gamma,b,c$, of the cosine of the scattering angle $z=\hat{\mathbf{k}}\cdot\hat{\mathbf{k}}'$ and pion velocity $v$ specified in the Appendix C, the imaginary part of the Compton scattering amplitude reads

$$[\mathrm{Im}R_1]^{\text{OPE-}\Delta}=C\Big\{(\alpha+z\gamma)(P_1P_2+P_3P_4)$$
$$+yA[P_1+(1-2d)P_2-(1+4d)P_4]$$
$$+y^2(1-2d)[\tfrac{1}{3}+(\tfrac{1}{2}-z)(A-\tfrac{1}{3})]$$
$$-\frac{y^2}{3}\,(P_2+2P_4)-\frac{y^3}{3}\Big\}, \tag{E7}$$

$$[\mathrm{Im}R_2]^{\text{OPE-}\Delta}=C\Big\{-\gamma(P_1P_2+P_3P_4)$$
$$+\frac{y^2}{2}\,(1-2d)(A-\tfrac{1}{3})\Big\},$$

$$[\mathrm{Im}R_3]^{\text{OPE-}\Delta}=C\{zP_6+(1-2z)P_7+(z^2-1)P_8\},$$

$$[\mathrm{Im}R_4]^{\text{OPE-}\Delta}=C\{P_6-P_7\},$$

$$[\mathrm{Im}R_5]^{\text{OPE-}\Delta}=C\{-P_6+\tfrac{3}{2}P_7-zP_8\},$$

$$[\mathrm{Im}R_6]^{\text{OPE-}\Delta}=C\{-\tfrac{1}{2}P_7+P_8\}.$$

Here

$$P_6=\alpha(f_1P_1-f_2P_3)+yf_1\left[A(1-2d)-\frac{y}{3}\right]+yf_2\left[A(1+4d)+\frac{2y}{3}\right],$$

$$P_7=vycP_1+y^2(\tfrac{1}{2}-d)(A-\tfrac{1}{3}),$$

$$P_8=\gamma(f_1P_1-f_2P_3)-vybP_1. \tag{E8}$$

Formulas (E7) specify the contribution of the OPE mechanism of the reaction $\gamma N\to\pi\Delta$ to the Compton scattering amplitude and we use them with two further modifications. First, we take into account a finite width of the $\Delta$ by virtue of smearing the contribution (E7) over the $\Delta$ mass $M$:

$$[\mathrm{Im}R_i(s,\theta)]^{\text{OPE-}\Delta}\to\int_{m+m_\pi}^{\infty}[\mathrm{Im}R_i(s,\theta,M)]^{\text{OPE-}\Delta}w(M)dM, \tag{E9}$$

where the integrand is given by formulas (E7). The weight $w(M)$ is

$$w(M)=\frac{2}{\pi\Gamma(M)}\sin^2\delta_{33}(M)\simeq\frac{2}{\pi}\frac{M_0^2\Gamma(M)}{(M^2-M_0^2)^2+M_0^2\Gamma^2(M)} \tag{E10}$$

and is determined by the energy-dependent width of the $\Delta$ isobar [86]:

$$\Gamma(M)=\Gamma_0\left(\frac{q'(M)}{q'(M_0)}\right)^3\frac{q'^2(M_0)+X^2}{q'^2(M)+X^2}, \tag{E11}$$

and by $M_0=1233$ MeV, $\Gamma_0=120$ MeV, and $X=185$ MeV. With the weight (E10), the integral (E9) exactly reproduces the OPE contribution of the three-body reaction $\gamma N\to\pi+(\pi' N)$ provided the $\pi N\to(\pi' N)$ block is taken on shell and contains only the $I=J=3/2$ partial wave.

Second, since the $\pi N\Delta$ vertex (E1) entering into Eq. (E4) includes a derivative and results in an increasing cross section at $s\to\infty$, we introduce a cutoff in the momentum transfer $t=(k-q)^2$ in the reaction $\gamma N\to\pi\Delta$. Namely, we replace the product of the propagators $(t-m_\pi^2)^{-1}(t'-m_\pi^2)^{-1}=(4qk\cdot qk'\cdot q)^{-1}$ in Eq. (E4) [here $t'=(k'-q)^2$] by

$$\frac{1}{(t-m_\pi^2)(t'-m_\pi^2)}\to\frac{1}{(t-m_\pi^2)(t'-m_\pi^2)}-\frac{1}{(t-\Lambda^2)(t'-\Lambda^2)}. \tag{E12}$$

This leads to a subtraction from $[\mathrm{Im}R_i]^{\text{OPE-}\Delta}$, Eq. (E7), a similar contribution obtained from (E7), (E6) through the substitutions

$$q_0\to q_{0\Lambda}=q_0+\frac{\Lambda^2-m_\pi^2}{2\omega},\quad d\to\frac{M^2+m^2-\Lambda^2}{2mM},$$

$$y\to\frac{\omega q_{0\Lambda}}{mM},\quad v\to\frac{q}{q_{0\Lambda}} \tag{E13}$$

($s,z,\omega,q,p_0,P_0$ are not changed). Such a subtraction is simpler for implementation than a straightforward use of adjusted form factors in the $\pi N\Delta$ vertices. At $\Lambda=0.5$ GeV the OPE cross section of $\gamma N\to\pi\Delta$ begins to decrease at $E_\gamma>1.2$ GeV.

In Fig. 7 we show the total photoabsorption cross section in the OPE approximation with $\Lambda=0.5$ GeV (dash-dotted curve). It is obtained from Im $R_i$ by using the optical theorem $\sigma_{\text{tot}}=(4\pi/\omega)\mathrm{Im}(R_1+R_2)_{\theta=0}$.

## APPENDIX F: CONTRIBUTION OF $\rho^0N$ INTERMEDIATE STATES

Considering contributions to Im$A_i$ from $\rho^0$ photoproduction we make the assumption of $s$-channel helicity conservation [58,55] in the reaction

$$\gamma+N\to\rho^0+N, \tag{F1}$$

so that

$$T_{\lambda_\rho\lambda',\lambda_\gamma\lambda}\sim\delta_{\lambda'\lambda}\delta_{\lambda_\rho\lambda_\gamma}\exp\left(\frac{B}{2}t_\rho\right), \tag{F2}$$

where $t_\rho=(p_\gamma-p_\rho)^2$ and the slope parameter $B\simeq 6$ GeV$^{-2}$ determines the angular dependence of the photoproduction amplitude. Using Eq. (F2) in the unitarity relation (B6) and integrating over transverse momenta we find that only the helicity-non-flip Compton scattering amplitudes $\tau_1$ and $\tau_2$ get a contribution from $\rho^0N$:

$$\mathrm{Im}[\tau_1]^{(\rho^0N)}=\mathrm{Im}[\tau_2]^{(\rho^0N)}=(s-m^2)\sigma_{\gamma N\to\rho^0N}(s)\exp\left(\frac{q}{2\omega}Bt\right), \tag{F3}$$

where $q$ and $\omega$ are the c.m. momenta of $\rho^0$ and $\gamma$ and $\sigma_{\gamma N\to\rho^0N}$ is the total cross section of the reaction (F1). Typically, $\sigma_{\gamma N\to\rho^0N}\sim 20-25$ $\mu$b at the energies considered here [58,55].

Note that the expression (F3) has a correct limit not only at high energies when the diffractive representation (F2) is experimentally justified but also near the $\rho N$ threshold where any angular dependence of the amplitudes Im $\tau_i$ on the $\gamma p$-scattering angle has to vanish.

Other mechanisms of low-energy $\rho$ photoproduction, like $\pi$ or $\sigma$ exchanges, could also be considered [97]. In spite of a very different spin structure inherent to these exchanges as compared with the above diffraction ansatz, the result for Im $\tau_i$ might be not so different. That is because both $\pi$ and $\sigma$ exchanges flip the helicity of the vector particles $\gamma\to\rho$, at least in the case of transversal polarizations of $\rho$, and thus result in diagonal helicity transitions $\gamma\to\gamma$ in the bilinear unitarity relation (B6).

## APPENDIX G: $s$-WAVE CORRECTION FOR $\pi\pi N$ INTERMEDIATE STATES

Considering the saturation of imaginary parts of the Compton scattering amplitudes, we have to discuss the rest of the total photoabsorption cross section, which is not covered by resonance excitation or peripheral mechanisms:

$$\Delta\sigma=[\sigma_{\gamma p\to\text{hadrons}}-\sigma_{\gamma p\to\pi N}]-[\sigma_{\gamma p\to N^*\to\pi\pi N}+\sigma^{\text{OPE}}_{\gamma p\to\pi\Delta}+\sigma_{\gamma N\to\rho^0 N}]. \quad \text{(G1)}$$

This quantity is shown in Fig. 7 (short-dashed line).

We can assume that the cross section $\Delta\sigma$ is dominated, at least at moderate energies, by electric dipole transitions. Moreover, an essential part of this cross section has to be related to the contact interaction in the $\gamma N\to\pi\Delta$ transition (analogous to the Kroll-Ruderman term in single-pion photoproduction) and hence to occur in states with angular momentum $j=3/2$. Under such assumptions it is easy to restore the corresponding contributions to all six Compton amplitudes because the $(E1,\ j=3/2)$ absorption has the same effect as the pion photoproduction through the multipole $E_{2-}$. Using formulas (B8) from Appendix B and the optical theorem $\text{Im}(\tau_1+\tau_2)_{\theta=0}=(s-m^2)\sigma_{\text{tot}}$, we may find Im $\tau_i$ through the following substitutions in Eqs. (B9):

$$\begin{aligned}
&8\pi q\sqrt{s}|A_{2-}|^2\to\tfrac{1}{8}x,\\
&8\pi q\sqrt{s}|B_{2-}|^2\to\tfrac{1}{2}x,\\
&8\pi q\sqrt{s}[A_{2-}B^*_{2-}]\to-\tfrac{1}{4}x,\quad x=(s-m^2)\Delta\sigma^{E1,j=3/2}
\end{aligned} \quad \text{(G2)}$$

(and other multipole amplitudes are replaced by zero).

When some part of the cross section $\Delta\sigma$ is caused by $E1$ absorption at $j=1/2$, that has the same effect on Im $\tau_i$ as the $E_{0+}$ multipole of single-pion photoproduction, and Im $\tau_i$ are found through the substitution

$$8\pi q\sqrt{s}|A_{0+}|^2\to(s-m^2)\Delta\sigma^{E1,j=1/2}. \quad \text{(G3)}$$

In the case of the $(M1,\ j=1/2)$ multipolarity which appears, for example, when both pions in the reaction $\gamma N\to\pi\pi N$ are produced in an $s$ wave, the substitution rule reads

$$8\pi q\sqrt{s}|A_{1-}|^2\to(s-m^2)\Delta\sigma^{M1,j=1/2}. \quad \text{(G4)}$$

Normally we assume that the whole cross section $\Delta\sigma$ is of $(E1,\ j=3/2)$ type, but with the above formulas we can also check what the effect is if a small amount of $\Delta\sigma$ is related to $(E1,\ j=1/2)$ or $(M1,\ j=1/2)$ quantum numbers.


[1] A. I. L'vov and V. A. Petrun'kin, in *Perspectives on Photon Interactions with Hadrons and Nuclei*, Vol. 365 of *Lecture Notes in Physics*, edited by M. Schumacher and G. Tamas (Springer-Verlag, Berlin, 1990), p. 123.

[2] V. A. Petrun'kin and A. I. L'vov, in *Proceedings of the 8th Seminar on Electromagnetic Interactions of Nuclei at Low and Medium Energies*, Moscow, 1991, edited by G. Gurevich (Institute for Nuclear Research, Moscow, 1992) p. 109.

[3] S. Capstick and B. D. Keister, Phys. Rev. D **46**, 84 (1992); **47**, 860 (1993).

[4] K. W. Rose *et al.*, Nucl. Phys. **A514**, 621 (1990).

[5] F. J. Federspiel *et al.*, Phys. Rev. Lett. **67**, 1511 (1991).

[6] A. Zieger *et al.*, Phys. Lett. B **278**, 34 (1992).

[7] B. E. Mac Gibbon *et al.*, Phys. Rev. C **52**, 2097 (1995).

[8] E. L. Hallin *et al.*, Phys. Rev. C **48**, 1497 (1993).

[9] G. Blanpied *et al.*, Phys. Rev. Lett. **76**, 1023 (1996).

[10] C. Molinari *et al.*, Phys. Lett. B **371**, 181 (1996).

[11] J. Peise *et al.*, Phys. Lett. B **384**, 37 (1996).

[12] F. V. Adamian *et al.*, J. Phys. G **19**, L193 (1993).

[13] V. I. Goldansky *et al.*, Nucl. Phys. **18**, 473 (1960).

[14] P. Baranov *et al.*, Phys. Lett. **52B**, 122 (1974).

[15] Yu. A. Alexandrov *et al.*, JETP Lett. **4**, 134 (1966).

[16] J. Schmiedmayer *et al.*, Phys. Rev. Lett. **66**, 1015 (1991).

[17] L. Koester *et al.*, Phys. Rev. C **51**, 3363 (1995).

[18] R. Weiner and W. Weise, Phys. Lett. **159B**, 85 (1985).

[19] F. Schöberl and H. Leeb, Phys. Lett. **166B**, 355 (1986).

[20] N. N. Scoccola and W. Weise, Nucl. Phys. **A517**, 495 (1990).

[21] V. S. Barashenkov and B. M. Barbashov, Nucl. Phys. **9**, 426 (1958).

[22] A. Kanazawa, Nucl. Phys. **24**, 524 (1961).

[23] V. A. Petrun'kin, Sov. J. Part. Nucl. **12**, 278 (1981).

[24] A. I. L'vov, Phys. Lett. B **304**, 29 (1993).

[25] B. R. Holstein and A. M. Nathan, Phys. Rev. D **49**, 6101 (1994).

[26] V. Bernard, N. Kaiser, and U.-G. Meissner, Nucl. Phys. **B373**, 346 (1992).

[27] V. Bernard, N. Kaiser, and U.-G. Meissner, Int. J. Mod. Phys. E **4**, 193 (1995).

[28] W. Broniowski and T. D. Cohen, Phys. Rev. D **47**, 299 (1993).

[29] E. N. Nikolov, W. Broniowski, and K. Goeke, Nucl. Phys. **A579**, 398 (1994).

[30] A. I. L'vov, Int. J. Mod. Phys. A **8**, 5267 (1993).

[31] R. A. Arndt, I. I. Strokovsky, and R. L. Workman, Phys. Rev. C **53**, 430 (1996); Computer code SAID, solution SM95, 1995.

[32] A. M. Sandorfi *et al.*, in *Excited Baryons*, edited by G. Adams *et al.* (World Scientific, Singapore, 1988), p. 256.

[33] T. Watabe, C. V. Christov, and K. Goeke, Phys. Lett. B **349**, 197 (1995).

[34] A. M. Sandorfi and M. Khandaker, Phys. Rev. Lett. **70**, 3835 (1993).

[35] S. Kabe *et al.*, Nucl. Phys. **B50**, 17 (1972).

[36] K. Toshioka *et al.*, Nucl. Phys. **B141**, 364 (1978).

[37] T. Ishii *et al.*, Nucl. Phys. **B165**, 189 (1980).

[38] Y. Wada *et al.*, Nuovo Cimento A **63**, 57 (1981).

[39] Y. Wada *et al.*, Nucl. Phys. **B247**, 313 (1984).

[40] T. Ishii *et al.*, Nucl. Phys. **B254**, 458 (1985).

[41] M. Jung *et al.*, Z. Phys. C **10**, 197 (1981).

[42] A. I. L'vov, Sov. J. Nucl. Phys. **34**, 597 (1981).

[43] A. I. L'vov, Sov. J. Nucl. Phys. **42**, 583 (1985).

[44] M. I. Levchuk, A. I. L'vov, and V. A. Petrun'kin, Few-Body Syst. **16**, 101 (1994).

[45] W. Pfeil, H. Rollnik, and S. Stankowski, Nucl. Phys. **B73**, 166 (1974).

[46] P. S. Baranov and L. V. Fil'kov, Sov. J. Part. Nucl. **7**, 42 (1976).
[47] I. Guiasu, C. Pomponiu, and E. E. Radescu, Ann. Phys. (N.Y.) **114**, 296 (1978).
[48] D. M. Akhmedov and L. V. Fil'kov, Sov. J. Nucl. Phys. **33**, 573 (1981).
[49] We should mention that there are examples of a different strategy when the dispersion relations do refer to the fundamental properties of hadrons. E.g., in applications to the chiral perturbation theory [24] or soliton physics [S. Saito and M. Uehara, Phys. Rev. D **51**, 6059 (1995)], they are used to find pion-loop contributions to polarizabilities of the nucleon in terms of the lowest-order chiral Lagrangian.
[50] G. Hida and M. Kikugawa, Prog. Theor. Phys. **55**, 1156 (1976); **58**, 372 (1977).
[51] V. Pascalutsa and O. Scholten, Nucl. Phys. **A591**, 658 (1995).
[52] M. Vanderhaeghen, Phys. Lett. B **368**, 13 (1996).
[53] O. Scholten *et al.*, report nucl-th/9604014, 1996.
[54] R. L. Walker, Phys. Rev. **182**, 1729 (1969).
[55] CBCG Collaboration, Phys. Rev. **163**, 1510 (1967); ABBHHMC Collaboration, *ibid.* **175**, 1669 (1968).
[56] P. Stichel and M. Scholz, Nuovo Cimento **34**, 1381 (1964); D. Lüke, M. Scheunert, and P. Stichel, Nuovo Cimento A **58**, 234 (1968).
[57] J. A. Gómez Tejedor and E. Oset, Nucl. Phys. **A571**, 667 (1994).
[58] J. Ballam *et al.*, Phys. Rev. D **5**, 545 (1972).
[59] T. A. Armstrong *et al.*, Phys. Rev. D **5**, 1640 (1972).
[60] M. MacCormick *et al.*, Phys. Rev. C **53**, 41 (1996).
[61] G. Buschhorn *et al.*, Phys. Lett. **37B**, 211 (1971).
[62] R. Workman and R. A. Arndt, Phys. Rev. D **45**, 1789 (1992).
[63] A. M. Sandorfi, C. S. Whisnant, and M. Khandaker, Phys. Rev. D **50**, R6681 (1995).
[64] J. Duda *et al.*, Z. Phys. C **17**, 319 (1983).
[65] V. V. Anisovich *et al.*, Phys. Lett. B **355**, 363 (1995).
[66] N. A. Törnqvist and M. Roos, Phys. Rev. Lett. **76**, 1575 (1996).
[67] M. Svec, Phys. Rev. D **53**, 2343 (1996).
[68] R. A. Arndt, R. L. Workman, and M. M. Pavan, Phys. Rev. C **49**, 2729 (1994).
[69] L. Montanet *et al.*, Particle Data Group, Phys. Rev. D **50**, 1173 (1994).
[70] M. V. Terent'ev, Sov. J. Nucl. Phys. **16**, 576 (1973).
[71] E. Witten, Nucl. Phys. **B223**, 422 (1983).
[72] M. Lutz and W. Weise, Nucl. Phys. **A518**, 156 (1990).
[73] The error in Eq. (21) is bigger than that in Eq. (20) because the first one includes uncertainties in the integral contribution to the difference of the polarizabilities, $(\overline{\alpha_p}-\overline{\beta_p})^{\rm int}\simeq(-1.8\pm2)\times10^{-4}$ fm$^3$.
[74] A. I. L'vov, Sov. J. Nucl. Phys. **34**, 289 (1981).
[75] A. Metz, diploma thesis, Mainz University, 1992.
[76] A. I. L'vov, V. A. Petrun'kin, and S. A. Startsev, Sov. J. Nucl. Phys. **29**, 651 (1979).
[77] J. Bernabeu, T. E. O. Ericson, and C. Ferro Fontan, Phys. Lett. **49B**, 381 (1974).
[78] V. Bernard *et al.*, Phys. Lett. B **319**, 269 (1993).
[79] P. A. M. Guichon, G. O. Liu, and A. W. Thomas, Nucl. Phys. **A591**, 606 (1995).
[80] R. F. Stiening, E. Loh, and M. Deutsch, Phys. Rev. Lett. **10**, 563 (1963).
[81] D. R. Rust *et al.*, Phys. Rev. Lett. **15**, 938 (1965).
[82] P. S. Baranov *et al.*, Sov. J. Nucl. Phys. **3**, 791 (1966); Sov. Phys. JETP **23**, 242 (1966).
[83] G. Barbellini, G. Capon, G. De Zorzi, and G. P. Murtas, Phys. Rev. **174**, 1665 (1968).
[84] M. Deutsch *et al.*, Phys. Rev. D **8**, 3828 (1973).
[85] H. Genzel, M. Jung, R. Wedemeyer, and H. J. Weyer, Z. Phys. A **279**, 399 (1976).
[86] W. J. Metcalf and R. Walker, Nucl. Phys. **B76**, 253 (1974).
[87] In attempts to reproduce the results of the isobar model of [37,39] we found that in these works the relative sign of the Born term and the resonance contribution was wrong, so that the background used there was actually minus the Born term times a form factor. In [39] this does not matter as far as the fit to the experimental data is concerned because there the relative phases of the background and the resonances were considered as adjustable parameters in each partial wave.
[88] G. K. Greenhut, Phys. Rev. D **1**, 1341 (1970).
[89] H. Falkenberg *et al.*, Nucl. Instrum. Methods Phys. Res. A **360**, 559 (1995).
[90] R. E. Prange, Phys. Rev. **110**, 240 (1958).
[91] A. A. Logunov and P. S. Isaev, Nuovo Cimento **10**, 917 (1958).
[92] A. C. Hearn, Nuovo Cimento **21**, 333 (1961).
[93] W. A. Bardeen and W. K. Tung, Phys. Rev. **173**, 1423 (1968).
[94] R. A. Arndt *et al.*, Phys. Rev. C **42**, 1864 (1990).
[95] B. Krusche *et al.*, Phys. Rev. Lett. **74**, 3736 (1995).
[96] M. Benmerrouche, N. C. Mukhopadhyay, and J. F. Zhang, Phys. Rev. D **51**, 3237 (1995).
[97] B. Friman and M. Soyeur, Nucl. Phys. **A600**, 477 (1996).